LA-10665-MS

UC-34C
Issued: May 1986

Cross Sections for Neutron-Producing Reactions Induced by 6- and 10-MeV Neutrons Incident on ^{10}B and ^{11}B

M. Drosg*
P. W. Lisowski
D. M. Drake
R. A. Hardekopf
S. M. Muellner**

LA--10665-MS

DE86 011734

*Consultant at Los Alamos. Department of Physics, University of Austria, Strudhofgasse A-1090, Ienat, AUSTRIA.
**Department of Physics, University of Austria, Strudhofgasse A-1090, Ienat, AUSTRIA.

Los Alamos National Laboratory
Los Alamos, New Mexico 87545

CROSS SECTIONS FOR NEUTRON-PRODUCING REACTIONS INDUCED BY 6- AND 10-MeV NEUTRONS INCIDENT ON ^{10}B AND ^{11}B

by

M. Drosg, P. W. Lisowski, D. M. Drake, R. A. Hardekopf, and M. Muellner

ABSTRACT

Using the time-of-flight technique, we have measured the ^{10}B and ^{11}B neutron emission spectra at incident neutron energies of 6.00 and 10.00 MeV for angles between 20^{o} and 145^{o}. Double differential cross sections and their integrated values have been extracted and are presented in tables and graphs. The integrated values (corrected for charged particle cross sections, if necessary) are in excellent agreement with measured total cross sections.

I. INTRODUCTION

Cross sections for neutron-induced reactions on light nuclei below about 14 MeV are important for fusion reactor design. Among these cross sections it is particularly difficult to measure nonelastic neutron cross sections because a monoenergetic neutron source of high yield is required to measure the resulting continuous spectra reliably. Between 8 and 14 MeV only the $^{1}H(t,n)^{3}He$ source has these required properties. Presently, the only installation that can supply bunched triton beams for fast neutron time-of-flight work are the Van de Graaffs of the Los Alamos National Laboratory. Consequently, double differential neutron cross sections of beryllium between 5.9 and 14.2 MeV, of lithium at 5.96 and 9.83 MeV, and of

^{6}Li, ^{7}Li, ^{10}B, ^{11}B, and carbon at 14.2 MeV have been measured[1-3] at the Los Alamos National Laboratory.

II. EXPERIMENTAL DETAILS

Bunched tritons from the tandem Van de Graaff at the Los Alamos National Laboratory were used to produce 6.00-MeV and 10.00-MeV neutrons by the $^{1}H(t,n)^{3}He$ reaction with full width at half maximum (FWHM) energy spreads of 0.15 MeV and 0.10 MeV, respectively. The target was a gas cell with an entrance foil of 5.3 mg/cm^2 molybdenum and a beamstop of 0.05 cm gold. The target to sample distance was 14.0 cm, the flight path 252.3 cm. The ^{10}B sample was a slightly irregularly shaped cylinder of 4 cm height, a purity of 95.5%, and a mass of 1.80 moles. During the data analysis it was discovered that the spectra were contaminated by peaks from elastic scattering from hydrogen. From the intensity of the peaks and the well-known cross sections[4] it was concluded that 0.31 $\pm$ 0.03 wt% of the sample was hydrogen. Consequently all relevant spectra were corrected for this contamination. The ^{11}B sample was a right-circular cylinder of about 3 cm height, 1.7 cm diameter, a purity of 90.5%, and a mass of 0.92 moles.

The general setup has been described before[1,2], as well as the measurement of the efficiency of the NE213 neutron detector[5] at the 0.3-MeV bias as used in this experiment.

The advantages of using the $^{1}H(t,n)^{3}He$ reaction at 0^{o} are threefold:

a) for 10-MeV neutrons this reaction is the only monoenergetic source. (The neutrons from the second line have 0.033 MeV and are, therefore, too low in energy to be a factor in this type of experiment.)

b) for 6-MeV neutrons the specific neutron yield is an order of magnitude larger than that of the competing p-T and d-D reactions (see Fig. 1).

c) the neutrons are emitted only into a forward cone, facilitating the source shadowing and giving smaller overall room background.

Although the t-H source is intrinsically monoenergetic, the background stemming from triton interactions with the target structure (entrance foil, beamstop) must be subtracted. Therefore, at each angle four neutron spectra must be measured[1]:

a) sample in, hydrogen gas in the cell

b) sample out, hydrogen gas in the cell

c) sample in, hydrogen removed from the cell

d) sample out, hydrogen removed from the cell.

The final spectrum is obtained (after appropriate normalization) by subtracting b) and c) from the sum of a) and d). However, this procedure is not exact, because in the "gas-in" spectra the neutron yield from the beam stop is lower than in the "gas-out" case because of the energy loss of the tritons in the gas. By scattering from hydrogen it was concluded that to a first order this difference can be taken into account by downscaling the "hydrogen-out" runs by 1.015 ± 0.005. In the present experiment six spectra were measured at each angle,because both "sample-out" runs are identical for the two samples. So, at each angle ^{10}B and ^{11}B were measured relative to each other.

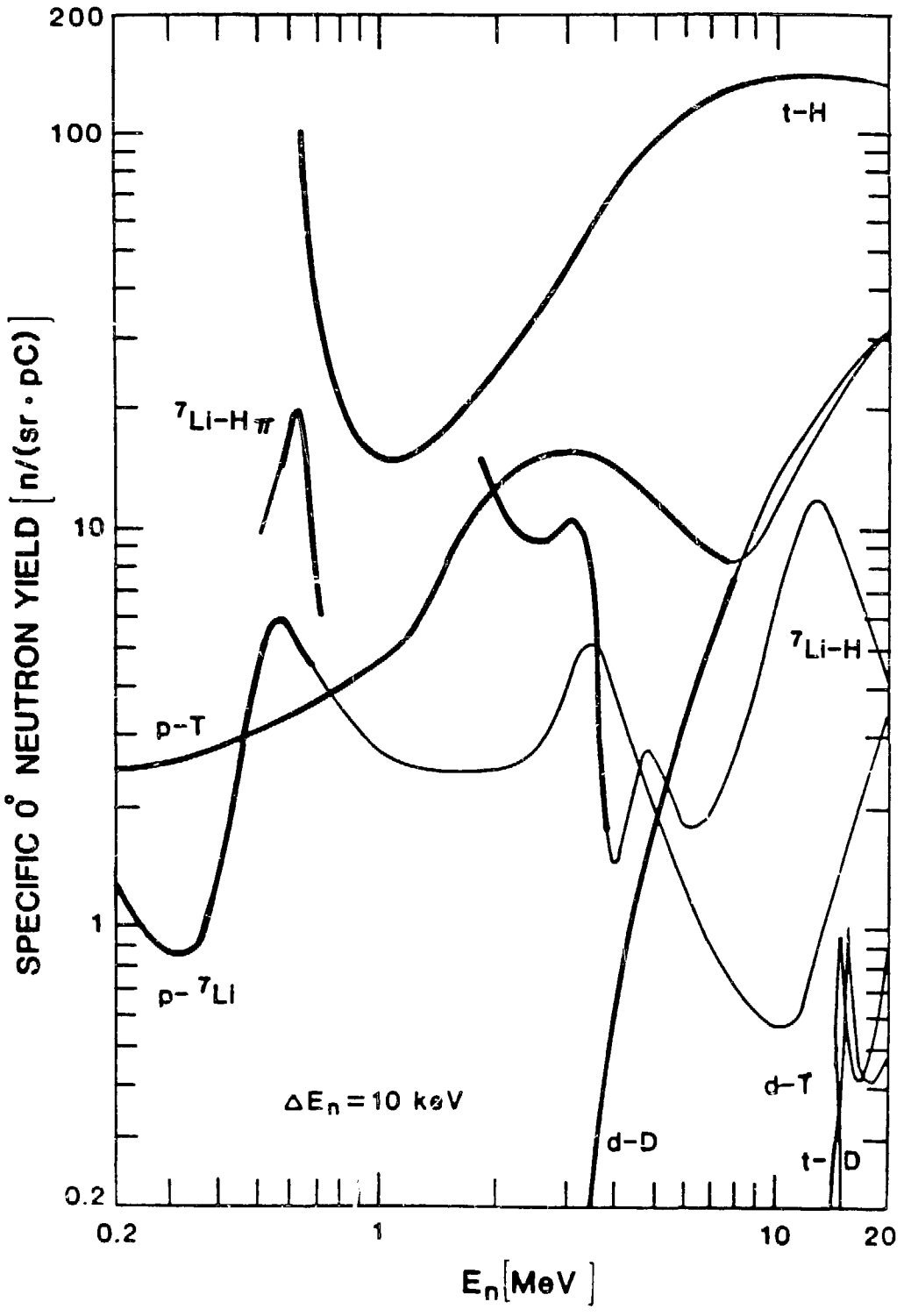

Fig. 1. Energy dependence of the specific zero-degree neutron yield. Except for d-T and t-D the thick curves indicate the monoenergetic range of the reaction in question. The index π denotes the second neutron group at 0° (180° in the c.m. system).

The use of a fast time digitizer[1] and a rather long spacing between the neutron bursts (800 ns) resulted in a dead time of less than 1%. After dead-time correction the six spectra at each angle were normalized by using the accumulated beam charge. The "gas-in" runs were, in addition, normalized to the accumulated counts of the neutron monitor viewing the gas target. After correcting for temperature and pressure changes in the active volume of the gas target, the two methods agreed to better than 0.5%.

At 35°, scattering from hydrogen (using cylindrical samples of 2.92 g polyethelene and 2.83 g carbon foam with a height of 2.54 cm and a diameter of 1.25 cm as foreground and background samples respectively) was used to obtain absolute cross sections by comparison with the $^{1}H(n,n)^{1}H$ cross section standard[4].

III. DATA REDUCTION

The normalized net time-of-flight spectra obtained the way described in Section II were converted (in a first order relativistic approximation) to energy spectra and corrected for the energy dependence of the neutron detection efficiency. Then, at each angle, the appropriate proportion of the spectrum of the other isotope was subtracted to correct for its admixture. This way the uncorrected spectra of Tables I through IV were obtained. These spectra were then corrected for multiple scattering using the Monte Carlo simulation performed by the Los Alamos National Laboratory code MCNP[6] (Tables V through VIII). For these calculations the cross section library ENDF/B-IV was used. In this simulation the scattered

TABLE I. Uncorrected Double Diff. Neutron Emission Cross Sections for 6.0-MeV Neutrons on ^{10}B [Data and Errors in mb/(sr*MeV)]

LAB.ANGLE [Deg]	20.0		25.0		35.0		45.0		60.0		75.0		90.0		110.0		130.0		145.0	
E-RANGE [MeV]																				
0.35-0.50	6.34	0.58	7.56	0.57	5.32	0.47	5.42	0.46	4.35	0.39	5.32	1.01	3.14	0.35	4.84	0.31	3.59	0.35	2.15	0.36
0.50-0.65	7.29	0.41	8.01	0.39	4.57	0.32	3.38	0.31	2.71	0.28	9.52	0.46	6.45	0.24	1.66	0.20	1.45	0.22	1.42	0.26
0.65-0.80	3.27	0.39	3.68	0.36	2.62	0.28	4.51	0.25	7.40	0.23	4.91	0.21	1.17	0.19	0.76	0.19	0.91	0.23	1.20	0.24
0.80-0.95	5.51	0.32	6.95	0.30	7.46	0.24	6.73	0.23	3.47	0.20	1.38	0.18	0.81	0.22	0.65	0.17	1.10	0.17	1.09	0.21
0.95-1.10	5.57	0.30	4.78	0.27	2.94	0.21	2.02	0.20	1.54	0.20	0.52	0.24	1.06	0.18	1.15	0.14	1.16	0.16	1.20	0.20
1.10-1.25	1.59	0.28	2.32	0.25	1.32	0.21	1.51	0.22	1.13	0.70	0.95	0.15	0.98	0.15	1.46	0.13	3.79	0.16	8.47	0.21
1.25-1.40	1.80	0.30	2.34	0.28	1.55	0.24	1.48	0.20	1.61	1.18	1.25	0.14	1.49	0.14	5.57	0.15	10.10	0.18	4.87	0.19
1.40-1.55	1.69	0.26	2.18	0.23	1.33	0.18	1.37	0.17	1.78	1.24	1.39	0.14	4.61	0.15	11.53	0.17	1.68	0.14	1.25	0.17
1.55-1.70	1.79	0.25	1.99	0.22	1.69	0.17	1.74	0.16	2.36	1.18	6.08	0.16	14.96	0.20	1.65	0.11	0.85	0.13	1.02	0.16
1.70-1.85	2.32	0.24	2.89	0.21	1.75	0.17	2.53	0.16	6.91	0.68	15.99	0.20	4.59	0.14	1.07	0.10	1.11	0.12	0.73	0.16
1.85-2.00	2.27	0.23	2.58	0.20	3.37	0.17	6.84	0.18	16.37	0.22	4.50	0.14	1.10	0.11	0.89	0.10	1.03	0.13	0.74	0.15
2.00-2.20	7.18	0.21	7.87	0.19	10.92	0.17	12.81	0.17	4.41	0.13	1.02	0.09	1.05	0.09	0.98	0.09	1.11	0.10	1.19	0.13
2.20-2.40	9.48	0.21	8.92	0.19	4.98	0.14	2.99	0.13	0.91	0.10	0.80	0.09	1.00	0.09	1.01	0.09	2.38	0.11	5.59	0.15
2.40-2.60	2.59	0.19	2.46	0.16	1.91	0.13	1.25	0.58	1.00	0.10	0.91	0.09	1.09	0.09	2.40	0.10	5.23	0.17	3.12	0.23
2.60-2.80	3.43	0.18	3.36	0.17	2.86	0.13	2.09	1.30	1.34	0.10	1.29	0.09	1.87	0.09	5.05	0.15	1.34	0.17	1.57	0.12
2.80-3.00	3.68	0.18	3.50	0.17	2.88	0.13	2.92	1.49	1.98	0.10	3.08	0.10	5.61	0.14	1.70	0.14	1.74	0.10	1.22	0.11
3.00-3.20	3.71	0.18	3.83	0.17	3.37	0.14	4.07	1.30	3.19	0.12	6.64	0.16	3.71	0.16	2.02	0.09	1.35	0.09	1.62	0.11
3.20-3.40	4.52	0.18	4.05	0.18	6.32	0.16	7.65	0.66	6.75	0.19	3.61	0.17	2.33	0.10	2.15	0.09	2.41	0.10	4.01	0.13
3.40-3.60	9.11	0.21	8.23	0.21	13.70	0.40	10.51	0.22	4.15	0.17	2.17	0.10	2.11	0.10	2.67	0.10	6.36	0.13	11.28	0.17
3.60-3.80	13.14	0.28	12.31	0.29	13.81	0.97	4.39	0.18	2.34	0.11	1.95	0.09	2.22	0.10	4.86	0.12	11.58	0.17	10.58	0.17
3.80-4.00	7.91	0.23	7.09	0.24	4.46	1.78	3.28	0.12	2.06	0.10	1.91	0.10	3.03	0.11	9.70	0.15	12.16	0.18	30.09	0.28
4.00-4.25	6.33	0.18	7.22	0.20	4.98	1.41	3.05	0.11	1.91	0.10	2.88	0.10	6.18	0.12	11.87	0.16	46.06	0.36	79.78	0.65
4.25-4.50	6.63	0.19	6.90	0.58	2.40	0.69	2.89	0.11	2.80	0.10	6.12	0.12	9.15	0.14	44.06	0.35	59.33	0.85	25.05	0.84
4.50-4.75	11.45	0.24	13.08	1.08	2.45	0.36	4.88	0.12	6.01	0.13	8.36	0.14	22.21	0.26	71.51	0.79	13.10	0.48	7.71	0.17
4.75-5.00	21.53	0.73	11.10	2.17	12.44	0.17	11.34	0.17	9.28	0.15	19.40	0.22	61.00	0.59	22.08	0.51	11.00	0.16	7.78	0.13
5.00-5.25	45.79	1.51	31.83	1.10	32.03	0.29	25.04	0.26	19.69	0.25	43.24	0.40	43.51	0.53	12.37	0.16	3.48	0.10		
5.25-5.50	99.35	2.46	80.77	0.83	90.32	0.68	68.62	0.55	45.69	0.46	28.96	0.38	14.49	0.19	2.79	0.08	0.40	0.06		
5.50-5.75	259.60	2.27	209.25	1.51	207.06	1.52	133.71	1.08	38.44	0.40	8.33	0.15	4.15	0.10	0.34	0.05	0.15	0.05		
5.75-6.00	406.55	3.24	363.19	2.90	181.65	1.73	74.96	0.87	7.84	0.14	1.31	0.07	0.37	0.06	0.05	0.04				
6.00-6.25	188.56	1.82	167.44	1.69	27.91	0.44	6.28	0.16	0.83	0.06	0.19	0.05	0.20	0.05						
6.25-6.50	17.14	0.27	10.06	0.19	1.76	0.08	0.49	0.06	0.05	0.05										
6.50-6.75	1.98	0.10	1.46	0.09	0.70	0.06	0.10	0.06												
6.75-7.00	0.88	0.09	0.72	0.08	0.24	0.06														

TABLE II. Uncorrected Double Diff. Neutron Emission Cross Sections for 10.0-MeV Neutrons on ^{10}B [Data and Errors in mb/(sr*MeV)]

LAB.ANGLE [Deg	20.0		35.0		45.0		60.0		75.0		90.0		110.0		130.0		145.0	
E-RANGE [MeV]																		
0.35- 0.50	5.23	1.69	8.48	1.61	1.88	1.23	7.61	1.35	2.34	1.13	2.89	0.98	3.52	1.03	2.57	0.97	3.91	1.16
0.50- 0.65	5.48	1.26	4.29	1.13	4.19	0.84	4.53	0.92	1.11	0.96	4.09	0.68	1.78	0.69	2.11	0.66	2.94	0.87
0.65- 0.80	5.29	1.12	5.66	0.98	2.72	0.73	3.60	0.79	2.03	0.82	3.33	0.58	2.05	0.59	1.81	0.58	2.16	0.80
0.80- 0.95	2.37	1.04	5.75	0.91	3.60	0.67	2.24	0.71	5.73	0.55	2.16	0.52	2.62	0.52	1.92	0.51	3.18	0.74
0.95- 1.10	4.08	0.97	4.18	0.83	4.28	0.61	3.29	0.64	4.78	0.50	2.28	0.47	2.68	0.47	2.44	0.46	2.05	0.68
1.10- 1.25	4.17	0.91	2.75	0.79	2.71	0.57	3.91	0.60	2.96	0.46	2.64	0.43	2.44	0.42	2.43	0.42	3.10	0.64
1.25- 1.40	3.31	0.85	4.51	0.72	4.31	0.52	3.00	0.55	2.05	0.42	3.11	0.40	1.63	0.39	3.21	0.39	3.61	0.60
1.40- 1.55	3.90	0.81	4.14	0.68	3.86	0.50	2.66	0.52	2.70	0.40	2.71	0.36	2.95	0.37	2.63	0.38	4.19	0.58
1.55- 1.70	1.62	0.79	3.85	0.67	2.73	0.48	3.62	0.49	2.64	0.37	3.20	0.35	3.50	0.35	6.19	0.39	6.65	0.58
1.70- 1.85	2.74	0.75	3.00	0.63	3.14	0.45	3.38	0.47	2.98	0.36	4.70	0.33	5.42	0.35	6.00	0.38	5.49	0.55
1.85- 2.00	1.86	0.72	3.52	0.60	3.17	0.43	6.09	0.46	3.80	0.34	4.66	0.31	6.96	0.35	7.50	0.37	17.44	0.55
2.00- 2.20	3.18	0.60	4.22	0.50	2.61	0.37	6.99	0.41	5.18	0.27	8.01	0.28	6.57	0.28	21.08	0.33	10.69	0.43
2.20- 2.40	1.72	0.58	3.36	0.49	4.78	0.36	5.45	0.63	7.58	0.27	6.32	0.25	22.53	0.31	5.04	0.26	2.23	0.38
2.40- 2.60	3.75	0.58	5.09	0.48	5.11	0.34	2.71	0.95	6.76	0.24	15.47	0.27	9.39	0.26	2.83	0.24	4.63	0.37
2.60- 2.80	5.27	0.56	5.88	0.47	5.40	0.36	4.40	0.77	12.54	0.25	20.33	0.28	3.33	0.22	4.18	0.23	5.19	0.35
2.80- 3.00	4.89	0.57	6.39	0.46	5.98	0.31	8.95	0.39	21.78	0.28	5.35	0.21	3.46	0.21	3.49	0.22	2.99	0.34
3.00- 3.20	5.55	0.52	6.11	0.42	6.98	0.30	21.50	0.34	7.72	0.23	3.12	0.20	3.70	0.20	2.49	0.22	1.13	0.34
3.20- 3.40	6.73	0.49	11.1-	0.41	18.46	0.33	13.09	0.31	2.60	0.20	2.82	0.19	2.17	0.20	0.85	0.19	0.17	0.34
3.40- 3.60	17.09	0.50	21.40	0.42	16.10	0.31	2.07	0.26	2.03	0.19	3.78	0.20	1.85	0.19	0.38	0.20	0.53	0.29
3.60- 3.80	21.93	0.50	12.12	0.38	3.56	0.26	1.40	0.24	3.44	0.19	2.15	0.19	0.04	0.18	0.56	0.18	2.03	0.27
3.80- 4.00	7.25	0.45	1.82	0.34	1.79	0.24	2.83	0.24	2.15	0.20	1.17	0.18	0.34	0.20	1.63	0.17	4.72	0.27
4.00- 4.25	2.98	0.38	2.78	0.29	5.22	0.22	2.97	0.22	1.72	0.17	0.48	0.17	0.80	0.15	3.04	0.16	1.79	0.22
4.25- 4.50	4.63	0.38	4.82	0.29	3.98	0.55	2.31	0.21	0.55	0.17	0.64	0.16	2.21	0.15	0.88	0.14	0.63	0.21
4.50- 4.75	7.37	0.38	4.02	0.28	1.25	0.78	1.08	0.20	0.46	0.16	1.12	0.14	1.19	0.15	0.33	0.13	0.52	0.20
4.75- 5.00	4.31	0.37	3.42	0.27	0.71	0.78	0.48	0.21	0.99	0.14	1.77	0.14	0.51	0.14	0.41	0.13	1.05	0.20
5.00- 5.25	5.11	0.37	2.38	0.28	1.04	0.55	1.14	0.18	2.15	0.14	0.93	0.14	0.48	0.14	0.56	0.13	1.14	0.20
5.25- 5.50	3.39	0.39	3.02	0.28	2.50	0.35	2.20	0.17	1.21	0.14	0.49	0.13	0.83	0.14	0.80	0.14	0.73	0.20
5.50- 5.75	4.56	0.34	5.01	0.25	4.59	0.19	2.37	0.17	0.61	0.13	0.68	0.13	1.04	0.14	0.69	0.14	0.96	0.18
5.75- 6.00	6.57	0.33	7.09	0.33	4.62	0.19	0.82	0.16	0.62	0.13	0.99	0.13	1.08	0.14	0.96	0.13	1.85	0.18
6.00- 6.25	8.93	0.34	7.46	0.52	2.73	0.18	0.68	0.16	0.74	0.13	1.27	0.14	1.25	0.13	1.43	0.13	2.75	0.18
6.25- 6.50	6.88	0.33	3.90	0.65	1.22	0.16	0.78	0.15	0.85	0.13	1.17	0.13	1.44	0.13	3.21	0.14	5.54	0.19
6.50- 6.75	4.72	0.33	1.66	0.77	0.94	0.16	0.65	0.16	1.20	0.13	1.38	0.13	3.31	0.15	6.49	0.17	7.57	0.21
6.75- 7.00	4.34	0.35	1.87	0.71	1.75	0.17	1.25	0.17	1.24	0.14	2.20	0.14	7.61	0.19	11.05	0.21	12.09	0.25
7.00- 7.25	5.46	0.37	2.63	0.53	1.56	0.17	1.40	0.17	1.31	0.14	4.96	0.17	13.92	0.24	17.56	0.25	10.02	0.25
7.25- 7.50	7.20	0.39	3.97	0.28	2.40	0.18	1.35	0.16	2.05	0.14	10.15	0.21	21.83	0.29	15.24	0.27	2.78	0.19
7.50- 7.75	10.07	0.42	3.79	0.24	2.25	0.17	1.93	0.16	4.22	0.16	14.75	0.24	30.18	0.34	4.40	0.19	1.39	0.16
7.75- 8.00	10.97	0.46	4.46	0.22	3.20	0.17	2.79	0.17	6.63	0.18	19.59	0.28	21.89	0.34	1.69	0.13	1.34	0.15
8.00- 8.30	17.79	0.58	9.24	0.23	7.55	0.19	6.18	0.18	9.75	0.19	27.58	0.32	6.91	0.21	1.92	0.12	1.31	0.13
8.30- 8.60	40.12	0.91	28.23	0.34	21.42	0.28	9.98	0.21	15.72	0.24	19.75	0.32	4.03	0.15	1.23	0.11	0.55	0.13
8.60- 8.90	93.37	1.48	62.75	0.51	39.00	0.39	13.04	0.23	15.57	0.26	6.36	0.19	2.56	0.13	0.16	0.10		
8.90- 9.20	144.61	1.33	74.68	0.59	38.51	0.38	16.44	0.25	6.27	0.17	3.11	0.13	0.64	0.10				
9.20- 9.50	169.78	1.37	92.22	0.66	52.88	0.44	13.38	0.23	2.36	0.12	0.93	0.10	0.14	0.09				
9.50- 9.80	253.89	1.78	140.86	0.95	65.42	0.57	5.57	0.18	0.55	0.10	0.21	0.10						
9.80-10.10	287.34	2.20	116.98	0.97	34.31	0.43	1.39	0.13	0.05	0.09								
10.10-10.40	142.49	1.46	37.17	0.48	5.28	0.17	0.09	0.12										
10.40-10.70	16.57	0.36	3.00	0.18	0.46	0.11												
10.70-11.00	2.12	0.20	0.63	0.15	0.27	0.11												
11.00-11.30	1.11	0.18	0.58	0.15														

TABLE III. Uncorrected Double Diff. Neutron Emission Cross Sections for 6.0-MeV Neutrons on ^{11}B [Data and Errors in mb/(sr*MeV)]

LAB.ANGLE [Deg]	20.0		25.0		35.0		45.0		60.0		75.0		90.0		110.0		130.0		145.0	
E-RANGE [MeV]																				
0.35-0.50	6.05	1.11	7.83	1.08	5.32	0.89	6.57	0.85	8.80	0.73	16.25	0.68	14.33	0.68	3.11	0.60	2.31	0.65	2.41	0.66
0.50-0.65	14.51	0.77	18.10	0.72	21.40	0.59	26.93	0.58	22.39	0.51	8.78	0.44	3.48	0.42	2.13	0.38	6.12	0.42	11.36	0.50
0.65-0.80	38.44	0.71	34.95	0.66	24.23	0.52	11.37	0.46	2.00	0.39	2.35	0.35	3.33	0.35	18.64	0.39	24.84	0.44	13.36	0.47
0.80-0.95	5.78	0.60	5.76	0.53	2.22	0.42	2.29	0.38	3.12	0.34	7.14	0.33	28.38	0.43	17.91	0.38	3.40	0.35	3.20	0.44
0.95-1.10	2.44	0.56	3.74	0.50	3.64	0.39	4.37	0.36	13.21	0.37	37.01	0.44	15.82	0.37	1.71	0.29	2.50	0.31	0.49	0.37
1.10-1.25	6.61	0.55	8.49	0.49	11.58	0.41	23.73	0.43	33.74	0.44	7.54	0.30	0.88	0.28	0.27	0.25	0.46	0.27	0.49	0.37
1.25-1.40	30.85	0.57	31.49	0.53	30.67	0.44	20.55	0.40	3.02	0.31	0.45	0.25	0.47	0.27	0.27	0.25	0.36	0.26	0.17	0.33
1.40-1.55	14.98	0.51	11.91	0.45	3.24	0.33	1.83	0.29	1.88	0.30	0.99	0.24	0.25	0.25	0.24	0.25	0.36	0.26	0.40	0.31
1.55-1.70	2.01	0.46	2.43	0.40	1.36	0.31	1.36	0.29	1.14	0.29	0.83	0.24	0.27	0.26	1.04	0.21	0.54	0.24	1.27	0.29
1.70-1.85	3.20	0.44	3.19	0.38	2.49	0.30	2.12	0.27	1.20	0.26	0.28	0.28	0.27	0.26	1.32	0.21	1.64	0.23	1.02	0.29
1.85-2.00	2.20	0.43	3.66	0.36	2.13	0.29	1.09	0.27	1.05	0.29	1.71	0.22	1.97	0.22	1.67	0.20	2.01	0.23	1.80	0.28
2.00-2.20	2.27	0.37	1.74	0.32	1.24	0.26	1.29	0.26	1.66	0.21	1.89	0.18	2.26	0.19	2.30	0.18	2.77	0.20	2.34	0.24
2.20-2.40	2.39	0.37	2.92	0.32	2.04	0.24	1.68	0.22	1.33	0.19	2.02	0.17	2.13	0.18	2.96	0.18	4.33	0.20	7.46	0.27
2.40-2.60	3.11	0.34	3.38	0.29	2.33	0.23	1.81	0.22	1.45	0.18	2.07	0.16	2.49	0.18	3.73	0.18	21.16	0.30	37.67	0.39
2.60-2.80	3.78	0.33	3.84	0.28	2.76	0.22	2.53	0.25	1.72	0.18	2.06	0.17	3.26	0.18	20.36	0.29	27.35	0.32	7.26	0.25
2.80-3.00	6.75	0.33	6.03	0.29	4.89	0.23	4.29	0.27	3.03	0.18	3.28	0.18	14.57	0.28	22.60	0.29	3.00	0.18	1.76	0.21
3.00-3.20	7.18	0.33	7.51	0.31	6.43	0.25	6.28	0.27	7.89	0.22	17.92	0.29	23.45	0.32	2.87	0.16	1.70	0.17	1.79	0.21
3.20-3.40	8.20	0.33	7.51	0.32	7.95	0.27	9.51	0.28	24.44	0.33	25.74	0.32	6.59	0.21	3.10	0.16	2.14	0.18	1.57	0.22
3.40-3.60	15.70	0.38	15.14	0.38	22.64	0.38	29.56	0.39	23.05	0.32	5.53	0.20	4.11	0.19	4.53	0.18	3.31	0.21	2.30	0.25
3.60-3.80	36.20	0.47	36.92	0.50	33.47	0.43	23.50	0.34	3.88	0.20	3.00	0.17	3.64	0.19	4.66	0.19	5.01	0.25	5.38	0.28
3.80-4.00	23.39	0.42	22.46	0.45	9.66	0.35	4.22	0.22	2.55	0.19	2.38	0.17	3.74	0.19	5.27	0.22	9.67	0.29	20.37	0.48
4.00-4.25	7.21	0.32	6.08	0.35	4.42	0.28	3.14	0.19	2.40	0.18	2.87	0.16	4.80	0.20	9.87	0.25	44.17	0.65	111.96	1.09
4.25-4.50	6.36	0.35	6.69	0.35	4.54	0.23	3.71	0.19	2.96	0.19	3.74	0.19	8.03	0.24	41.93	0.63	160.21	1.01	166.94	0.81
4.50-4.75	6.47	0.44	6.68	0.37	5.32	0.22	3.69	0.20	3.96	0.20	6.61	0.23	29.85	0.44	141.58	1.07	91.91	0.58	20.34	0.31
4.75-5.00	11.92	0.63	10.97	0.42	8.62	0.29	6.51	0.26	8.27	0.25	19.43	0.37	97.28	0.93	96.11	0.63	7.91	0.25	3.07	0.20
5.00-5.25	35.28	0.99	26.29	0.55	30.37	0.52	23.30	0.44	27.35	0.41	54.42	0.67	89.49	0.78	10.12	0.26	1.34	0.14	0.61	0.12
5.25-5.50	130.43	1.71	98.34	1.12	108.71	1.18	78.54	0.95	69.59	0.73	57.88	0.57	12.32	0.30	1.38	0.13	0.28	0.10		
5.50-5.75	347.65	3.34	266.53	2.56	275.77	2.51	187.63	1.73	57.77	0.64	11.53	0.25	1.53	0.14	0.14	0.09				
5.75-6.00	614.44	4.87	548.63	4.35	326.24	2.31	156.29	1.16	7.81	0.22	1.15	0.11	0.08	0.09						
6.00-6.25	344.24	2.42	317.98	2.22	77.25	0.60	16.78	0.29	0.66	0.11	0.04	0.08								
6.25-6.50	36.67	0.43	19.97	0.33	3.64	0.15	0.92	0.12	0.12	0.09										
6.50-6.75	3.51	0.18	2.12	0.16	1.48	0.12	0.56	0.11												
6.75-7.00	1.73	0.16	1.36	0.15																
7.00-7.25	0.57	0.14																		

TABLE IV. Uncorrected Double Diff. Neutron Emission Cross Sections for 10.0-MeV Neutrons on ^{11}B [Data and Errors in mb/(sr*MeV)]

LAB.ANGLE [Deg]	20.0		35.0		45.0		60.0		75.0		90.0		110.0		130.0		145.0	
E-RANGE [MeV]																		
0.35- 0.50	5.83	3.09	12.43	2.91	2.77	2.24	0.21	2.65	2.42	1.84	2.01	1.74	1.67	2.08	-0.15	1.46	3.65	2.10
0.50- 0.65	8.76	2.27	0.74	1.96	0.60	1.46	1.43	1.88	2.77	1.21	1.75	1.14	0.41	1.52	0.09	1.48	3.92	1.57
0.65- 0.80	5.59	2.00	2.85	1.67	5.28	1.24	3.24	1.37	0.21	1.02	0.28	0.97	1.71	1.00	0.90	1.12	1.94	1.49
0.80- 0.95	14.64	1.84	12.72	1.53	3.21	1.31	0.09	1.23	1.55	0.93	1.57	0.89	2.41	0.99	0.08	1.12	0.22	1.67
0.95- 1.10	12.11	1.75	0.35	1.45	0.75	1.27	0.08	1.24	1.69	0.88	3.48	0.87	0.07	0.94	0.06	0.91	1.63	1.49
1.10- 1.25	0.53	1.72	0.35	1.45	0.11	1.07	0.87	1.16	5.16	0.83	0.59	0.80	0.39	0.81	5.29	0.82	15.35	1.22
1.25- 1.40	2.57	1.56	0.23	1.32	2.95	0.96	4.25	0.99	1.73	0.76	1.57	0.74	7.72	0.76	7.25	0.76	3.44	1.14
1.40- 1.55	5.78	1.46$	6.38	1.24	9.68	0.89	0.61	0.95	1.11	0.74	4.55	0.71	11.55	0.74	1.93	0.71	12.87	1.10
1.55- 1.70	11.99	1.42	6.70	1.18	1.34	0.86	0.75	0.89	3.66	0.68	17.16	0.70	2.22	0.67	23.88	0.73	21.84	1.06
1.70- 1.85	4.37	1.33	0.51	1.08	1.19	0.78	1.38	0.83	17.56	0.69	4.14	0.63	14.31	0.67	12.39	0.66	1.53	0.98
1.85- 2.00	2.92	1.26	2.37	1.01	3.88	0.74	14.07	0.82	7.89	0.64	4.89	0.60	19.70	0.65	1.45	0.60	1.13	0.95
2.00- 2.20	3.29	1.05	6.28	0.87	14.35	0.68	10.15	0.73	4.22	0.52	16.99	0.53	0.35	0.54	0.19	0.53	0.91	0.77
2.20- 2.40	12.81	1.07	16.79	0.90	7.49	0.66	4.95	0.64	17.77	0.52	3.22	0.45	0.05	0.56	1.09	0.45	1.81	0.71
2.40- 2.60	10.07	1.01	4.33	0.80	7.08	0.59	20.37	0.63	4.80	0.47	0.11	0.44	0.62	0.43	1.18	0.41	2.26	0.67
2.60- 2.80	11.30	0.95	19.26	0.78	30.20	0.63	6.80	0.56	0.27	0.44	0.79	0.44	1.69	0.39	2.05	0.40	3.32	0.65
2.80- 3.00	41.93	0.97	29.84	0.77	8.81	0.54	0.44	0.52	0.12	0.45	1.18	0.37	2.37	0.37	5.61	0.40	17.56	0.66
3.00- 3.20	16.64	0.88	2.46	0.67	0.50	0.50	0.05	0.59	1.46	0.38	2.49	0.35	3.66	0.36	17.74	0.44	8.69	0.62
3.20- 3.40	1.80	0.83	1.08	0.66	0.12	0.52	0.62	0.55	1.58	0.35	1.37	0.34	12.79	0.41	7.89	0.39	17.12	0.62
3.40- 3.60	1.88	0.83	0.64	0.67	1.22	0.49	1.32	0.46	1.92	0.34	6.07	0.36	9.33	0.38	18.82	0.44	18.90	0.61
3.60- 3.80	3.06	0.82	1.95	0.61	1.45	0.44	1.89	0.43	4.74	0.35	11.29	0.38	12.10	0.39	13.75	0.40	1.22	0.52
3.80- 4.00	2.82	0.76	2.02	0.56	2.05	0.42	3.59	0.44	11.46	0.39	7.64	0.36	21.03	0.43	1.47	0.32	1.27	0.50
4.00- 4.25	3.35	0.66	2.54	0.50	3.43	0.38	10.84	0.42	9.50	0.34	17.59	0.37	4.49	0.31	0.66	0.28	0.46	0.43
4.25- 4.50	5.87	0.66	8.18	0.51	13.87	0.42	12.51	0.41	16.99	0.37	12.26	0.34	1.08	0.28	0.57	0.27	0.48	0.41
4.50- 4.75	18.84	0.68	18.70	0.53	17.44	0.43	15.77	0.41	15.70	0.36	1.17	0.27	0.71	0.27	0.96	0.26	1.18	0.39
4.75 5.00	22.50	0.67	15.74	0.51	17.07	0.42	21.13	0.44	1.48	0.27	0.79	0.26	0.85	0.26	1.57	0.26	2.83	0.38
5.00- 5.25	23.90	0.67	27.37	0.55	28.32	0.47	5.00	0.35	0.97	0.26	0.73	0.25	1.12	0.25	2.99	0.26	6.49	0.40
5.25- 5.50	40.53	0.70	24.52	0.53	8.02	0.37	0.85	0.32	0.26	0.25	1.31	0.25	2.47	0.26	7.80	0.30	11.90	0.41
5.50- 5.75	14.25	0.63	3.06	0.43	0.83	0.33	0.20	0.31	1.17	0.25	2.12	0.25	4.71	0.28	11.84	0.32	5.25	0.36
5.75- 6.00	3.12	0.59	1.38	0.43	0.80	0.32	0.38	0.30	1.01	0.25	3.67	0.26	9.99	0.31	3.74	0.26	0.87	0.33
6.00- 6.25	2.82	0.58	2.28	0.43	1.14	0.32	1.06	0.29	2.08	0.25	5.38	0.27	7.19	0.28	0.84	0.23	0.46	0.32
6.25- 6.50	4.63	0.57	2.28	0.42	1.56	0.3	1.61	0.30	2.93	0.26	7.02	0.28	1.80	0.24	1.74	0.24	2.50	0.32
6.50- 6.75	5.03	0.59	2.94	0.43	2.18	0.31	2.51	0.31	5.34	0.28	4.24	0.26	2.58	0.26	4.23	0.28	5.66	0.35
6.75- 7.00	6.63	0.62	4.48	0.45	4.41	0.33	4.80	0.34	5.51	0.28	2.21	0.25	5.95	0.31	8.42	0.33	11.86	0.41
7.00- 7.25	11.06	0.67	6.49	0.46	5.82	0.34	6.96	0.35	2.35	0.26	3.58	0.28	13.93	0.40	14.35	0.41	19.69	0.45
7.25- 7.50	11.21	0.69	9.90	0.46	10.26	0.36	4.68	0.32	1.81	0.25	7.99	0.33	21.09	0.48	25.09	0.46	16.91	0.41
7.50- 7.75	16.79	0.74	14.00	0.46	9.30	0.35	2.07	0.29	3.70	0.26	14.76	0.39	30.15	0.57	20.53	0.39	4.19	0.31
7.75- 8.00	15.92	0.80	10.04	0.41	4.40	0.31	2.49	0.29	7.34	0.30	21.08	0.45	40.53	0.56	5.58	0.27	1.24	0.26
8.00- 8.30	8.08	0.90	6.81	0.38	4.55	0.30	5.64	0.30	11.95	0.33	33.40	0.54	26.31	0.40	1.31	0.20	0.77	0.24
8.30- 8.60	14.82	1.30	19.32	0.56	14.74	0.45	10.25	0.36	18.61	0.41	42.37	0.54	4.62	0.26	0.61	0.20	0.28	0.24
8.60- 8.90	69.36	1.88	51.10	0.93	35.31	0.66	13.02	0.39	26.82	0.45	16.94	0.36	1.16	0.21	0.27	0.19		
8.90- 9.20	139.19	2.29	73.61	1.07	37.99	0.65	17.40	0.41	14.85	0.33	2.36	0.22	0.58	0.18				
9.20- 9.50	158.20	2.59	83.91	1.24	46.25	0.78	19.01	0.40	3.08	0.21	0.42	0.18	0.38	0.17				
9.50- 9.80	239.69	3.50	135.85	1.79	74.52	0.98	9.66	0.32	0.51	0.19	0.23	0.18						
9.80-10.10	363.60	3.76	150.89	1.61	55.49	0.70	2.41	0.26										
10.10-10.40	249.26	2.08	64.82	0.77	11.80	0.33	0.18	0.21										
10.40-10.70	41.58	0.60	6.67	0.33	0.44	0.21												
10.70-11.00	4.33	0.36	0.62	0.28	0.72	0.20												
11.00-11.30	1.24	0.32	0.66	0.27														
11.30-11.60	1.69	0.32																

TABLE V. Corrected Double Diff. Neutron Emission Cross Sections for 6.0-MeV Neutrons on ^{10}B [Data and Errors in mb/(sr*MeV)]

LAB.ANGLE [Deg]	20.0		25.0		35.0		45.0		60.0		75.0		90.0		110.0		130.0		145.0	
E-RANGE [MeV]																				
0.35-0.50	8.7	1.5	10.6	2.6	8.6	2.1	7.9	1.4	5.9	0.9	6.3	1.2	2.5	0.4	6.1	0.8	4.3	0.6	2.8	0.5
0.50-0.65	7.5	0.5	8.4	0.6	3.8	0.5	7.1	2.0	5.6	1.6	12.1	1.5	8.1	0.9	1.2	0.3	1.0	0.3	1.0	0.3
0.65-0.80	3.2	0.4	3.7	0.4	1.3	0.7	8.4	2.1	10.5	1.6	7.7	1.5	3.2	1.1	0.1	0.4	0.3	0.3	0.6	0.3
0.80-0.95	9.6	2.3	11.6	3.8	11.3	2.3	7.2	0.4	3.8	0.3	1.7	0.3	0.9	0.2	0.5	0.2	0.9	0.2	0.9	0.2
0.95-1.10	11.0	3.0	10.9	4.9	8.3	3.3	1.4	0.3	1.0	0.3	0.04	0.3	0.6	0.3	1.2	0.2	1.1	0.2	1.1	0.2
1.10-1.25	3.2	1.0	4.3	1.6	2.9	1.0	1.1	0.3	0.7	0.7	0.9	0.2	0.9	0.1	2.1	0.4	4.2	0.3	8.9	0.4
1.25-1.40	1.4	0.4	2.1	0.3	1.1	0.3	1.1	0.3	1.2	1.2	1.5	0.2	1.6	0.2	6.5	0.6	10.8	0.5	5.6	0.5
1.40-1.55	1.1	0.4	1.7	0.4	0.7	0.4	1.3	0.2	1.7	1.2	2.2	0.5	5.2	0.4	12.0	0.3	2.0	0.3	1.6	0.3
1.55-1.70	1.1	0.4	1.3	0.5	0.9	0.4	2.0	0.2	2.5	1.2	7.4	0.8	16.0	0.7	1.6	0.1	0.8	0.1	1.0	0.2
1.70-1.85	2.0	0.3	2.6	0.2	1.4	0.2	3.4	0.6	7.6	0.8	16.8	0.5	5.2	0.4	0.9	0.1	0.9	0.1	0.7	0.2
1.85-2.00	2.5	0.3	3.0	0.5	3.5	0.3	8.7	1.1	17.9	0.9	4.6	0.2	1.1	0.1	0.4	0.2	0.6	0.2	0.7	0.2
2.00-2.20	8.5	0.8	9.4	1.4	12.2	0.9	14.0	0.7	5.4	0.6	0.8	0.1	0.8	0.1	0.7	0.1	0.8	0.1	1.5	0.3
2.20-2.40	12.0	1.4	11.8	2.4	7.5	1.6	3.3	0.3	1.2	0.2	0.4	0.2	0.5	0.2	1.0	0.1	2.1	0.1	6.2	0.6
2.40-2.60	3.3	0.6	3.5	1.0	2.7	0.6	0.9	0.6	0.6	0.1	0.4	0.2	1.1	0.1	3.4	0.6	5.9	0.5	3.3	0.3
2.60-2.80	3.6	0.3	3.7	0.5	3.0	0.3	1.5	1.3	1.0	0.1	0.8	0.1	2.3	0.4	5.9	0.6	2.0	0.5	1.6	0.2
2.80-3.00	2.9	0.3	2.7	0.3	2.0	0.3	2.1	1.5	1.8	0.2	2.8	0.2	6.8	0.9	1.9	0.3	2.0	0.3	0.9	0.1
3.00-3.20	2.6	0.3	2.9	0.3	3.0	0.2	3.6	1.3	3.8	0.7	7.3	0.7	4.0	0.6	1.5	0.2	1.2	0.2	1.2	0.2
3.20-3.40	3.4	0.3	3.3	0.2	6.3	0.5	7.5	0.7	7.6	0.8	4.5	0.9	2.2	0.4	1.3	0.2	2.0	0.2	3.5	0.2
3.40-3.60	8.7	0.4	8.8	1.1	15.4	1.6	12.0	1.2	4.0	0.4	2.3	0.5	1.1	0.2	1.7	0.3	5.3	0.5	9.8	0.6
3.60-3.80	14.1	1.0	13.8	1.8	14.9	1.4	5.4	0.9	2.0	0.3	1.5	0.3	1.3	0.2	3.9	0.5	12.7	0.3	10.4	0.3
3.80-4.00	10.1	1.6	9.4	2.4	5.0	1.9	3.8	0.6	1.6	0.2	1.0	0.2	2.1	0.3	8.8	0.6	15.2	0.6	31.0	0.3
4.00-4.25	7.5	0.9	8.2	1.2	4.9	1.4	2.5	0.2	1.1	0.2	1.9	0.3	5.4	0.7	16.3	0.9	59.2	2.7	90.9	2.3
4.25-4.50	6.7	0.4	7.0	0.7	1.9	0.7	2.6	0.3	2.0	0.3	5.3	0.7	12.8	0.7	58.0	2.8	64.8	1.4	30.9	1.4
4.50-4.75	11.3	0.3	12.9	1.1	2.1	0.4	4.9	0.5	5.4	0.5	9.4	0.5	31.3	1.8	84.3	2.7	13.6	0.5	9.3	0.4
4.75-5.00	21.5	0.9	11.8	2.3	12.3	0.6	12.2	0.7	9.5	0.6	23.7	0.8	73.8	2.6	26.2	1.0	9.9	0.3	7.4	0.2
5.00-5.25	45.4	1.8	36.0	1.9	31.7	1.1	28.7	0.7	23.4	0.7	51.6	1.7	49.8	1.4	11.5	0.2	3.4	0.1		
5.25-5.50	145.1	9.3	120.0	7.7	112.0	4.2	83.8	3.1	53.2	1.6	33.0	0.9	14.7	0.2	2.6	0.1	0.4	0.1		
5.50-5.75	345.3	17.2	275.3	13.2	248.4	8.3	154.0	4.2	43.9	1.2	9.2	0.2	3.8	0.1	0.3	0.05	0.1	0.05		
5.75-6.00	496.7	18.3	431.4	13.9	225.5	8.9	93.2	3.7	10.2	0.5	0.8	0.1	0.3	0.1	0.1	0.04				
6.00-6.25	239.7	10.4	208.0	8.3	53.1	5.1	15.0	1.8	0.5	0.1	0.2	0.05	0.2	0.05						
6.25-6.50	17.0	0.3	13.0	0.6	1.8	0.1	0.5	0.1	0.05	0.05										
6.50-6.75	1.9	0.1	2.1	0.2	0.7	0.1	0.1	0.1												
6.75-7.00	0.9	0.1	0.7	0.1	0.2	0.1														

TABLE VI. Corrected Double Diff. Neutron Emission Cross Sections for 10.0-MeV Neutrons on ^{10}B [Data and Errors in mb/(sr*MeV)]

LAB.ANGLE [Deg]	20.0		35.0		45.0		60.0		75.0		90.0		110.0		130.0		145.0	
E-RANGE [MeV]																		
0.35- 0.50	4.5	1.7	7.9	1.6	1.7	1.2	7.7	1.4	2.9	1.2	2.9	1.0	3.5	1.0	3.0	1.0	4.1	1.2
0.50- 0.65	4.9	1.3	3.9	1.1	4.3	0.9	4.8	0.9	1.7	1.0	3.7	0.7	1.7	0.7	2.4	0.7	3.2	0.9
0.65- 0.80	5.3	1.1	5.9	1.0	3.5	0.9	3.9	0.8	1.9	0.8	3.2	0.6	2.4	0.6	1.7	0.6	2.0	0.8
0.80- 0.95	3.5	1.2	6.5	1.0	3.4	0.7	2.3	0.7	6.1	0.6	2.5	0.6	2.6	0.5	2.1	0.6	3.4	0.8
0.95- 1.10	4.3	1.0	4.4	0.9	4.0	0.6	3.7	0.7	4.8	0.5	2.4	0.5	2.8	0.5	2.5	0.5	2.1	0.7
1.10- 1.25	3.8	0.9	2.8	0.8	2.7	0.6	4.2	0.6	2.8	0.5	2.7	0.5	2.6	0.5	2.5	0.4	3.3	0.7
1.25- 1.40	2.8	0.9	4.8	0.8	4.8	0.6	2.6	0.6	1.7	0.4	3.4	0.5	1.6	0.4	3.6	0.5	4.2	0.7
1.40- 1.55	4.8	1.0	4.2	0.7	3.4	0.5	2.2	0.5	3.0	0.5	2.6	0.4	3.2	0.5	2.5	0.4	4.3	0.6
1.55- 1.70	1.6	0.8	3.8	0.7	2.3	0.5	3.7	0.5	2.7	0.4	3.4	0.4	3.4	0.4	6.1	0.4	7.3	0.7
1.70- 1.85	2.3	0.8	3.2	0.7	3.1	0.5	3.6	0.5	3.1	0.4	4.8	0.4	5.2	0.4	6.1	0.4	7.2	1.1
1.85- 2.00	1.3	0.7	4.5	0.8	3.7	0.6	6.0	0.5	4.3	0.5	4.2	0.3	7.0	0.4	8.1	0.6	20.5	1.8
2.00- 2.20	4.4	0.9	3.8	0.5	2.8	0.4	7.6	0.6	4.8	0.3	7.8	0.3	7.2	0.6	24.2	1.8	11.5	0.7
2.20- 2.40	1.4	0.6	3.2	0.5	5.7	0.7	5.2	0.6	7.2	0.3	6.5	0.4	25.9	1.9	5.4	0.4	1.4	0.5
2.40- 2.60	3.7	0.6	6.8	1.1	5.0	0.3	2.4	1.0	7.2	0.5	17.8	1.4	10.4	0.8	2.2	0.3	4.2	0.4
2.60- 2.80	7.4	1.4	5.8	0.5	5.3	0.4	5.2	1.0	14.9	1.4	24.9	2.5	2.6	0.3	4.6	0.4	6.5	0.8
2.80- 3.00	5.9	0.9	6.4	0.5	6.6	0.6	11.0	1.3	26.2	2.4	6.2	0.6	3.5	0.2	4.3	0.5	3.9	0.6
3.00- 3.20	6.4	0.8	6.8	0.7	8.8	1.1	25.8	2.4	9.5	1.1	2.6	0.3	4.8	0.7	3.2	0.5	0.8	0.3
3.20- 3.40	6.7	0.6	14.3	1.9	22.7	2.4	15.6	1.5	2.0	0.3	3.3	0.4	3.0	0.5	0.9	0.2	0.2	0.4
3.40- 3.60	20.6	2.1	27.7	3.4	19.4	1.9	1.9	0.3	2.3	0.3	4.9	0.7	1.9	0.3	0.1	0.2	0.3	0.3
3.60- 3.80	29.7	4.2	16.0	2.1	4.0	0.4	1.5	0.3	4.6	0.7	3.0	0.6	0.1	0.2	0.2	0.2	2.3	0.3
3.80- 4.00	10.9	2.0	1.9	0.4	1.3	0.3	3.9	0.6	3.0	0.6	1.3	0.2	0.0	0.2	1.9	0.3	5.7	0.6
4.00- 4.25	2.6	0.4	3.0	0.4	5.9	0.5	4.1	0.7	2.2	0.4	0.2	0.2	0.8	0.2	3.9	0.5	2.0	0.3
4.25- 4.50	5.6	0.7	6.3	0.9	5.3	1.0	3.0	0.5	0.5	0.2	0.4	0.2	3.0	0.5	1.0	0.2	0.4	0.2
4.50- 4.75	9.3	1.2	5.6	1.0	2.2	1.0	1.0	0.2	0.3	0.2	1.4	0.2	1.8	0.4	0.1	0.2	0.4	0.2
4.75- 5.00	5.9	1.0	4.3	0.6	1.0	0.8	0.1	0.2	1.2	0.2	2.8	0.6	0.4	0.1	0.4	0.1	1.1	0.2
5.00- 5.25	5.4	0.5	2.3	0.3	0.7	0.6	1.3	0.3	2.7	0.4	1.1	0.3	0.3	0.1	0.7	0.2	1.4	0.3
5.25- 5.50	3.0	0.4	2.7	0.3	2.3	0.4	2.7	0.4	1.5	0.3	0.1	0.2	0.7	0.2	1.0	0.2	0.9	0.2
5.50- 5.75	4.2	0.3	5.1	0.3	4.9	0.4	2.9	0.4	0.4	0.2	0.3	0.1	1.0	0.2	0.6	0.2	0.9	0.2
5.75- 6.00	6.8	0.5	7.8	0.7	5.3	0.6	0.9	0.2	0.3	0.1	0.9	0.2	1.0	0.2	0.6	0.1	1.6	0.2
6.00- 6.25	9.9	0.8	8.3	0.8	3.0	0.4	0.4	0.2	0.6	0.2	1.4	0.3	1.0	0.2	1.1	0.2	2.4	0.2
6.25- 6.50	7.7	0.7	4.2	0.7	1.1	0.2	0.6	0.2	0.9	0.2	1.1	0.2	1.0	0.2	2.7	0.2	5.5	0.2
6.50- 6.75	4.9	0.4	1.5	0.8	0.7	0.2	0.7	0.2	1.3	0.3	1.0	0.2	2.7	0.2	6.9	0.2	8.8	0.3
6.75- 7.00	4.1	0.4	1.7	0.7	1.7	0.2	1.5	0.3	1.1	0.2	1.6	0.2	8.2	0.2	13.3	0.5	14.7	0.6
7.00- 7.25	5.3	0.4	2.7	0.5	1.7	0.3	1.4	0.3	0.7	0.2	4.1	0.3	17.2	0.7	21.6	0.9	11.4	0.4
7.25- 7.50	7.3	0.4	4.3	0.4	2.6	0.3	1.1	0.2	1.4	0.2	10.1	0.2	27.6	1.2	17.1	0.5	3.0	0.2
7.50- 7.75	10.5	0.5	4.1	0.4	2.2	0.2	1.5	0.2	3.4	0.3	17.3	0.5	36.3	1.3	4.3	0.2	1.1	0.2
7.75- 8.00	11.4	0.5	4.6	0.3	3.0	0.2	2.3	0.2	6.7	0.2	24.8	1.1	25.8	0.8	1.1	0.2	1.2	0.1
8.00- 8.30	17.8	0.6	9.0	0.3	7.1	0.2	6.0	0.2	11.7	0.4	34.9	1.5	7.9	0.3	1.8	0.1	1.3	0.1
8.30- 8.60	39.6	0.9	27.6	0.4	20.7	0.3	11.4	0.3	19.3	0.7	24.2	0.9	3.7	0.2	1.2	0.1	0.6	0.1
8.60- 8.90	93.7	1.5	70.8	1.6	44.8	1.2	16.1	0.6	18.0	0.5	7.3	0.3	2.5	0.1	0.2	0.1		
8.90- 9.20	161.3	3.5	92.6	3.6	50.9	2.5	19.4	0.6	7.0	0.2	2.8	0.1	0.6	0.1				
9.20- 9.50	216.4	9.4	123.4	6.2	70.8	3.6	14.2	0.3	1.8	0.2	0.9	0.1	0.1	0.1				
9.50- 9.80	326.1	14.5	174.2	6.7	76.7	2.3	5.2	0.2	0.3	0.1	0.2	0.1						
9.80-10.10	363.5	15.4	138.8	4.5	37.4	0.8	1.1	0.1										
10.10-10.40	195.1	10.6	48.7	2.4	5.1	0.2	0.1	0.1										
10.40-10.70	39.2	4.5	3.7	0.2	0.4	0.1												
10.70-11.00	5.6	0.7	0.6	0.2	0.3	0.1												
11.00-11.30	1.1	0.2	0.6	0.1														

TABLE VII. Corrected Double Diff. Neutron Emission Cross Sections for 6.0-MeV Neutrons on ^{11}B [Data and Errors in mb/(sr*MeV)]

LAB.ANGLE [Deg]	20.0		25.0		35.0		45.0		60.0		75.0		90.0		110.0		130.0		145.0	
E-RANGE [MeV]																				
0.35-0.50	4.2	1.9	6.1	1.9	3.7	1.6	7.6	1.4	9.7	1.4	17.3	1.2	13.1	0.9	3.1	0.6	2.0	0.7	1.7	0.7
0.50-0.65	13.8	0.9	17.4	0.9	20.7	0.8	27.9	1.1	23.2	1.1	10.5	1.7	1.9	1.0	3.1	0.8	6.8	0.8	11.7	0.6
0.65-0.80	40.2	1.9	36.3	1.7	25.6	1.4	9.6	1.5	0.4	1.8	3.0	0.8	3.6	0.5	22.4	2.3	28.2	2.5	16.1	1.7
0.80-0.95	4.6	1.1	4.9	0.8	1.1	0.9	3.3	1.1	3.9	1.2	12.4	5.1	33.1	3.1	17.7	0.4	2.9	0.5	2.2	0.6
0.95-1.10	4.1	1.9	5.8	2.4	4.8	1.4	9.8	5.0	17.8	5.6	39.3	2.3	17.9	1.4	0.2	0.5	1.5	0.6	0.3	0.5
1.10-1.25	13.7	6.9	15.5	7.4	17.3	5.3	29.7	5.5	38.7	5.9	7.9	0.5	1.3	0.4	0.2	0.5	0.1	0.5	0.1	0.4
1.25-1.40	46.0	14.3	45.5	14.4	43.1	11.2	23.4	2.7	4.9	2.2	0.1	0.6	0.1	0.3	0.0	0.3	0.3	0.3	0.2	0.3
1.40-1.55	20.1	4.9	17.6	5.9	7.5	3.8	1.8	0.3	1.6	0.4	0.7	0.2	0.2	0.3	0.2	0.3	0.3	0.3	0.4	0.3
1.55-1.70	3.4	1.5	4.3	2.1	2.6	1.2	1.2	0.3	0.9	0.3	0.7	0.2	0.2	0.3	1.0	0.2	0.5	0.2	1.2	0.3
1.70-1.85	2.8	0.6	3.0	0.4	2.1	0.4	1.8	0.4	0.9	0.4	0.0	0.3	0.1	0.3	1.2	0.2	1.5	0.2	0.9	0.3
1.85-2.00	1.7	0.6	3.1	0.6	1.7	0.5	0.7	0.4	0.7	0.5	1.3	0.4	1.6	0.3	1.4	0.2	1.8	0.2	1.6	0.3
2.00-2.20	1.7	0.6	1.2	0.6	0.7	0.5	0.8	0.5	1.2	0.5	1.4	0.5	1.7	0.3	1.7	0.3	2.1	0.4	1.8	0.3
2.20-2.40	1.9	0.6	2.4	0.6	1.6	0.4	1.2	0.4	0.9	0.5	1.5	0.4	1.5	0.4	2.2	0.4	4.8	0.6	7.5	0.4
2.40-2.60	2.7	0.5	2.9	0.5	1.8	0.4	1.4	0.4	1.0	0.5	1.6	0.4	1.8	0.4	4.2	0.4	24.8	2.8	40.3	1.8
2.60-2.80	3.1	0.5	3.1	0.5	2.2	0.4	2.0	0.4	1.2	0.5	1.5	0.5	3.7	0.4	23.4	1.9	27.7	0.5	7.6	0.4
2.80-3.00	5.5	0.5	4.8	0.5	3.8	0.4	3.3	0.4	2.3	0.4	4.1	1.1	16.8	1.6	23.2	0.5	2.4	0.4	1.4	0.3
3.00-3.20	5.1	0.6	5.5	0.7	4.6	0.5	4.6	0.5	8.4	1.7	20.0	2.8	24.5	1.2	2.2	0.3	1.6	0.2	1.7	0.2
3.20-3.40	5.7	0.7	5.3	0.6	5.7	0.7	9.8	1.7	26.5	3.8	25.9	1.5	5.1	0.4	1.9	0.3	1.8	0.2	1.6	0.2
3.40-3.60	16.0	2.2	15.6	2.5	22.9	1.9	32.2	3.8	23.4	1.8	4.1	0.3	2.0	0.4	2.5	0.4	1.8	0.4	1.6	0.3
3.60-3.80	39.7	5.1	40.2	5.2	36.6	4.3	24.1	1.9	2.7	0.3	1.6	0.3	1.7	0.4	2.2	0.5	2.1	0.6	2.5	0.6
3.80-4.00	24.6	2.7	23.9	3.1	10.6	2.3	2.7	0.4	1.5	0.3	1.0	0.3	1.6	0.5	2.3	0.6	5.3	0.9	14.2	1.3
4.00-4.25	5.9	0.4	5.0	0.5	3.1	0.4	1.9	0.3	1.3	0.3	1.4	0.3	2.2	0.6	5.8	0.9	46.0	0.7	118.4	1.7
4.25-4.50	5.3	0.4	5.1	0.4	3.4	0.3	2.6	0.3	1.8	0.3	2.0	0.4	4.7	0.7	42.6	0.6	172.9	2.7	179.8	2.7
4.50-4.75	5.3	0.5	5.5	0.4	4.1	0.3	2.3	0.3	2.5	0.4	5.5	0.3	32.7	0.7	159.7	3.8	99.8	1.7	22.1	0.5
4.75-5.00	10.4	0.7	9.4	0.5	6.9	0.4	4.6	0.5	6.6	0.4	21.5	0.6	114.2	3.5	109.7	2.8	7.6	0.3	2.7	0.2
5.00-5.25	32.2	1.2	24.7	0.6	31.3	0.5	22.6	0.5	29.5	0.6	60.7	1.4	96.3	1.6	8.8	0.4	1.3	0.1	0.6	0.1
5.25-5.50	137.8	2.3	111.7	2.9	129.8	4.4	88.7	2.2	75.1	1.3	62.5	1.1	10.9	0.4	1.2	0.1	0.3	0.1		
5.50-5.75	393.9	9.8	312.8	9.6	317.6	8.7	209.8	4.8	63.1	1.2	12.7	0.3	0.9	0.2	0.1	0.1				
5.75-6.00	703.5	18.5	618.8	14.7	361.6	7.4	176.1	4.1	10.2	0.5	0.9	0.1								
6.00-6.25	403.4	12.1	359.8	8.7	89.9	2.6	24.3	1.5	0.4	0.1										
6.25-6.50	56.9	4.1	32.2	2.5	3.2	0.2	0.9	0.1	0.1	0.1										
6.50-6.75	3.5	0.2	2.1	0.2	1.5	0.1	0.6	0.1												
6.75-7.00	1.7	0.2	1.4	0.1																
7.00-7.25	0.6	0.1																		

TABLE VIII. Corrected Double Diff. Neutron Emission Cross Sections for 10.0-MeV Neutrons on ^{118} [Data and Errors in mb/(sr*MeV)]

LAB.ANGLE [Deg]	20.0		35.0		45.0		60.0		75.0		90.0		110.0		130.0		145.0	
E-RANGE [MeV]																		
0.35- 0.50	6.0	3.1	12.5	2.9	2.9	2.2	0.3	2.7	2.5	1.8	2.0	1.7	1.7	2.1	-0.1	1.5	3.7	2.1
0.50- 0.65	9.0	2.3	0.9	2.0	0.7	1.5	1.5	1.9	2.8	1.2	1.8	1.1	0.4	1.5	0.2	1.5	4.0	1.6
0.65- 0.80	5.5	2.0	2.8	1.7	5.3	1.2	3.2	1.4	0.2	1.0	0.3	1.0	1.7	1.0	0.9	1.1	2.0	1.5
0.80- 0.95	14.7	1.8	12.8	1.5	3.3	1.3	0.2	1.2	1.6	0.9	1.6	0.9	2.4	1.0	0.2	1.1	0.4	1.7
0.95- 1.10	12.2	1.8	0.5	1.5	0.9	1.3	0.2	1.2	1.8	0.9	3.5	0.9	0.2	0.9	0.2	0.9	1.8	1.5
1.10- 1.25	0.8	1.8	0.5	1.5	0.3	1.1	1.0	1.2	5.3	0.8	0.7	0.8	0.5	0.8	5.5	0.8	15.5	1.2
1.25- 1.40	2.9	1.7	0.4	1.3	3.1	1.0	4.4	1.0	1.8	0.8	1.6	0.7	7.8	0.8	7.4	0.8	3.7	1.2
1.40- 1.55	6.1	1.5	6.6	1.3	9.8	0.9	0.7	1.0	1.2	0.7	4.6	0.7	11.7	0.7	2.1	0.7	13.1	1.1
1.55- 1.70	12.2	1.5	6.9	1.2	1.5	0.9	0.9	0.9	3.8	0.7	17.2	0.7	2.3	0.7	24.0	0.7	21.9	1.1
1.70- 1.85	4.6	1.4	0.7	1.1	1.3	0.8	1.5	0.8	17.7	0.7	4.2	0.6	14.3	0.7	12.5	0.7	1.7	1.0
1.85- 2.00	3.2	1.3	2.5	1.0	4.0	0.8	14.2	0.8	8.0	0.6	4.9	0.6	19.6	0.6	[illegible]	0.6	1.4	1.0
2.00- 2.20	3.5	1.1	6.4	0.9	14.4	0.7	10.2	0.7	4.3	0.5	17.1	0.5	0.4	0.6	0.3	0.6	1.1	0.8
2.20- 2.40	12.8	1.1	16.8	0.9	7.6	0.7	5.2	0.7	17.9	0.5	3.3	0.5	0.1	0.6	1.1	0.5	1.9	0.7
2.40- 2.60	10.8	1.5	4.8	0.9	7.4	0.7	20.5	0.7	4.9	0.5	0.1	0.4	0.6	0.4	1.3	0.4	2.4	0.7
2.60- 2.80	11.8	1.2	19.5	0.8	30.4	0.7	6.9	0.6	0.3	0.5	0.8	0.5	1.7	0.4	2.2	0.4	3.5	0.7
2.80- 3.00	42.1	1.0	29.9	0.8	8.9	0.6	0.5	0.5	0.2	0.5	1.2	0.4	2.4	0.4	5.7	0.4	17.8	0.7
3.00- 3.20	16.8	1.0	2.6	0.7	0.6	0.5	0.2	0.6	1.6	0.4	2.5	0.4	3.7	0.4	17.9	0.5	8.9	0.7
3.20- 3.40	2.1	1.0	1.3	0.7	0.3	0.6	0.8	0.6	1.7	0.4	1.4	0.4	12.9	0.4	8.1	0.4	17.4	0.7
3.40- 3.60	2.3	1.1	0.9	0.7	1.4	0.5	1.5	0.5	2.0	0.4	6.1	0.4	9.4	0.4	19.1	0.5	19.3	0.8
3.60- 3.80	3.3	1.0	2.1	0.7	1.6	0.5	2.1	0.5	4.9	0.4	11.4	0.4	12.3	0.4	14.1	0.5	1.6	0.7
3.80- 4.00	3.2	1.0	2.3	0.7	2.3	0.5	3.8	0.5	11.6	0.4	7.8	0.4	21.3	0.5	1.7	0.4	1.6	0.6
4.00- 4.25	3.9	1.1	2.9	0.6	3.7	0.5	11.1	0.5	9.8	0.4	17.8	0.4	4.7	0.4	0.9	0.4	0.8	0.6
4.25- 4.50	6.4	1.1	8.6	0.7	14.3	0.6	12.9	0.5	17.2	0.4	12.4	0.4	1.2	0.3	0.9	0.4	0.9	0.7
4.50- 4.75	19.6	1.3	19.2	0.8	17.9	0.6	16.1	0.5	15.9	0.4	1.4	0.3	0.9	0.3	1.3	0.4	1.6	0.6
4.75- 5.00	23.0	1.2	16.1	0.7	17.3	0.5	21.4	0.5	1.7	0.3	1.0	0.3	1.1	0.3	1.9	0.4	3.2	0.6
5.00- 5.25	24.1	0.9	27.5	0.7	28.5	0.6	5.2	0.5	1.2	0.3	0.8	0.3	1.3	0.3	3.2	0.3	6.8	0.5
5.25- 5.50	40.9	1.1	24.7	0.7	8.2	0.5	1.1	0.5	0.4	0.3	1.3	0.3	2.6	0.3	8.0	0.4	12.2	0.6
5.50- 5.75	14.8	1.3	3.4	0.7	1.1	0.5	0.4	0.5	1.3	0.3	2.0	0.3	4.7	0.3	12.1	0.4	5.6	0.6
5.75- 6.00	3.8	1.5	1.7	0.8	1.0	0.5	0.5	0.5	1.1	0.3	3.5	0.3	9.9	0.4	3.9	0.4	1.3	0.6
6.00- 6.25	3.4	1.4	2.6	0.7	1.3	0.5	1.2	0.4	2.1	0.3	5.2	0.3	7.1	0.4	1.0	0.4	0.7	0.6
6.25- 6.50	5.2	1.3	2.5	0.7	1.7	0.5	1.8	0.4	3.0	0.3	6.9	0.3	1.7	0.4	1.8	0.4	2.6	0.6
6.50- 6.75	5.5	1.3	3.3	0.7	2.4	0.5	2.7	0.5	5.4	0.3	4.1	0.3	2.4	0.4	4.5	0.4	5.9	0.6
6.75- 7.00	7.2	1.4	4.8	0.8	4.6	0.5	5.0	0.5	5.6	0.4	2.0	0.4	5.5	0.4	9.1	0.4	12.5	0.6
7.00- 7.25	11.7	1.4	6.8	0.7	6.1	0.5	7.2	0.5	2.4	0.4	3.2	0.4	14.6	0.4	15.5	0.7	20.8	0.9
7.25- 7.50	11.8	1.2	10.2	0.7	10.5	0.5	4.9	0.5	1.8	0.3	7.4	0.4	23.2	0.7	26.4	0.8	17.3	0.5
7.50- 7.75	17.4	1.3	14.4	0.7	9.6	0.5	2.2	0.5	3.5	0.4	14.8	0.4	33.7	1.0	21.2	0.5	4.1	0.3
7.75- 8.00	16.6	1.5	10.5	0.8	4.7	0.5	2.6	0.5	7.1	0.4	22.7	0.5	43.7	0.9	5.7	0.3	1.0	0.3
8.00- 8.30	8.9	1.7	7.2	0.8	4.7	0.5	5.6	0.5	12.6	0.4	37.0	0.9	27.7	0.5	1.1	0.2	0.7	0.2
8.30- 8.60	15.4	1.9	19.5	0.8	14.7	0.6	10.6	0.5	20.2	0.6	46.0	0.9	4.6	0.3	0.5	0.2	0.3	0.2
8.60- 8.90	69.1	2.3	53.5	1.1	37.4	0.9	14.1	0.6	29.0	0.8	18.4	0.5	1.0	0.2	0.3	0.2		
8.90- 9.20	144.5	2.8	80.6	1.7	42.4	1.2	19.0	1.0	15.9	0.5	2.3	0.2	0.5	0.2				
9.20- 9.50	178.4	4.8	97.2	2.9	53.1	1.8	19.9	0.6	3.2	0.2	0.3	0.2	0.4	0.2				
9.50- 9.80	272.6	7.4	152.5	3.7	80.1	1.6	9.9	0.4	0.3	0.2	0.2	0.2						
9.80-10.10	405.9	9.2	163.1	2.9	58.1	0.9	2.2	0.3										
10.10-10.40	279.6	6.4	72.1	1.6	12.7	0.4	0.1	0.2										
10.40-10.70	56.8	3.1	8.2	0.4	0.3	0.2												
10.70-11.00	7.3	0.7	0.6	0.3	0.7	0.2												
11.00-11.30	1.2	0.3	0.7	0.3														
11.30-11.60	1.7	0.3																

neutrons were tallied by energy and angle according to the reaction types that created them: single elastic, double elastic, elastic-inelastic, single inelastic, double inelastic, and inelastic-elastic processes. As can be seen in the spectra shown in the Appendix this simulation does not stand up to reality. In many cases the scale of the inelastic portion is grossly too low; for ^{11}B at 10 MeV not even the shape of the spectrum is properly simulated. Consequently, also the simulated multiple scattering corrections are expected to be equally poor. Since an improvement of the cross section library ENDF/B-IV was not within the scope of this work, the following procedure is believed to give a first order improvement: the elastic and the inelastic portions of the simulated spectra were so adjusted that their integrals agreed with those of the corresponding portions of the measured spectra, changing the original simulation (shown as dotted curves in the figures of the Appendix) to the piecewise adjusted solution (dashed curves). The same adjustment factors were then applied to the corrections, i.e., their energy shape remained unchanged. Because of the sometimes very poor agreement in shape, the corrections were then done additively rather than in the usual multiplicative way.

IV. RESULTS

A. *Double Differential Cross Sections*

Tables V through VIII give the multiple scattering corrected double differential cross sections. Because the quality of the experiment is much better than that of the correction and a remeasurement is unlikely because of its complexity, it seems prudent to present both corrected and uncorrected data in numerical form. The former can be used to improve the

data base for a better multiple scattering correction which can then be applied to the uncorrected data. It is interesting to note that for both energies and both isotopes, practically all levels that can be excited are actually seen in the spectra, whereas only a few have been seen before[7,8] in neutron scattering experiments. This is possible because of the much more intense neutron source used in this experiment. However, no attempt was made to evaluate the inelastic differential cross sections of the individual levels because the multiple scattering correction is so unreliable.

B. *Differential Elastic Cross Sections*

The multiple scattering correction of the elastically scattered neutrons is expected to be quite reliable. Therefore, differential cross sections for the elastic scattering were extracted. In the case of ^{10}B, scattering involving the first excited state at 0.72 MeV could not be separated from the elastic scattering. Therefore, in Table IX we give cross sections of the highest energy peak rather than elastic cross sections.

In addition to the measured data, zero-degree and integrated cross sections as obtained by Legendre fitting (see Sec. C) are included in this table. In addition we have listed Wick's limit σ_W, the lower limit for the elastic 0^o cross section. Its center-of-mass value is derived from the total reaction cross section σ_T by

$$\frac{d\sigma}{d\Omega}(0^o) \geq \sigma_W = (k \frac{\sigma_T}{4\pi})^2 \quad ,$$

TABLE IX

ABSOLUTE DIFFERENTIAL LABORATORY CROSS SECTIONS OF THE HIGHEST ENERGY PEAK

Isotope	^{10}B				^{11}B			
Energy	6.0 MeV		10.0 MeV		6.0 MeV		10.0 MeV	
ANGLE [deg]	SIGMA [mb/sr]	ERROR [%]	SIGMA [mb/sr]	ERROR [%]	SIGMA [mb/sr]	ERROR [%]	SIGMA [mb/sr]	ERROR [%]
measured data:								
20.0	331.0	2.2	435.2	1.8	437.2	1.4	429.3	1.0
25.0	277.8	2.0			369.4	1.3		
35.0	171.9	2.0	206.8	1.6	236.7	1.3	195.3	0.9
45.0	98.7	1.7	94.5	1.6	132.7	1.3	91.1	1.0
60.0	37.2	1.5	22.9	1.4	47.5	1.0	25.7	2.1
75.0	33.8	1.8	20.4	1.6	41.8	1.1	27.2	1.3
90.0	48.6	1.9	35.4	1.7	65.6	1.5	43.3	1.0
110.0	52.8	2.0	33.9	1.6	82.9	1.5	40.9	1.1
130.0	45.0	1.8	17.6	1.7	83.7	1.0	21.5	1.6
145.0	46 1	1.6	12.3	1.9	84.5	1.0	16.4	2.6
calculated data:								
0.0	435.9		667.3		573.3		631.2	
Wick's limit	414 [a]		637 [a]		504		615	
integrated	927 mb [b]		844 mb [b]		1331 mb		876 mb	

a) using present value of the total cross section

b) according to ENDF/B-V, inelastic scattering from the first excited state (0.72 MeV) contributes 3% at 6 MeV and 1% at 10 MeV to this integrated value

where k is the center-of-mass wave number of the incoming neutron. Because of the quadratic dependence on σ_T, uncertainties in this quantity affect σ_W very strongly. In our case we took σ_T of ^{11}B from Reference 9 and that of ^{10}B from our present results, diminishing the effect of the scale uncertainty.

C. *Integrated Cross Sections*

The angular distributions of the energy integrated spectra are given in Table X. These data contain extrapolations to zero neutron energy. To account for events below the neutron detection bias, the following simple procedure was believed to be good enough considering the poor quality of the multiple scattering correction: it was assumed that the spectrum below the cutoff at 0.35 MeV was in the average as intense as the spectrum between 0.35 and 2.0 MeV. By assigning a 50% error to this extrapolation most eventualities should be taken care of.

The integration of the double differential cross sections over both the energy of the emitted neutrons and the solid angle was done in two steps. First, the cross section of the highest energy peak was converted into the center-of-mass system and integrated over the solid angle in this system, and then, the remaining spectrum was integrated over the energy and over the solid angle in the laboratory system.

The integrations over the solid angle were done by fitting the angular distributions by means of Legendre polynomials P_i so that the integrated cross section was obtained from the first coefficient A_o after multiplying by 4π.

TABLE X

ABSOLUTE DIFFERENTIAL NEUTRON EMISSION CROSS SECTIONS

Isotope	^{10}B				^{11}B			
Energy	6.0 MeV		10.0 MeV		6.0 MeV		10.0 MeV	
ANGLE [deg]	SIGMA [mb/sr]	ERROR [%]	SIGMA [mb/sr]	ERROR [%]	SIGMA [mb/sr]	ERROR [%]	SIGMA [mb/sr]	ERROR [%]
measured data:								
20.0	357.8	2.0	490.3	1.6	489.3	1.7	521.8	1.1
25.0	306.2	1.9			422.0	1.9		
35.0	195.8	1.9	251.8	1.5	279.7	1.8	262.1	1.1
45.0	118.8	1.7	127.9	1.5	171.2	1.9	145.5	1.8
60.0	52.9	1.9	52.2	2.1	80.1	2.9	63.4	2.1
75.0	48.6	2.0	46.2	2.1	71.3	2.9	61.7	1.8
90.0	60.5	2.0	60.1	2.3	90.8	1.9	75.7	1.6
110.0	61.7	1.9	54.7	2.3	104.2	1.5	73.2	1.7
130.0	52.6	1.7	36.4	2.7	105.0	1.3	53.6	2.1
145.0	53.0	2.6	32.5	2.6	103.5	1.5	52.3	2.6
calculated data:								
0.0	469.4		730.5		634.1		738.3	
integrated	1097 mb		1187 mb		1685 mb		1396 mb	

The advantage of the two step procedure lies in the smaller number of coefficients needed in the center-of-mass presentation of the elastic cross section, so that for the limited number of experimental points the fit (and its extrapolation to 0^{o} and 180^{o}) becomes more reliable. After removal of the strongly forward peaked elastic cross sections, the remaining data can be fitted even in the laboratory system with only a few coefficients.

Table XI collects all Legendre coefficients obtained in the present work. For convenience, the Legendre coefficients for describing the angular distribution of the total neutron emission in the laboratory system are also given. The latter fit was obtained under the following three constraints: A_o was fixed to the sum of the first coefficient of the elastic and that of the inelastic distribution, and the zero-degree and the 180-degree cross sections were taken to be the sum of the corresponding (extrapolated) values of the partial fits.

V. UNCERTAINTIES

A. *Energy and Angle*

The structure in the energy dependence and the rather strong angular dependence of the cross sections require a good knowledge both of the mean neutron energy and the scattering angle. For this work, the spread of the incoming energy was assumed to be rectangular, and the angular spread was disregarded. The incoming neutron energy is uncertain by 0.03 MeV, the zero degree direction by 0.4^{o}. Compared to the latter, the individual uncertainty of each angle is unimportant (0.1^{o}).

TABLE XI

LEGENDRE COEFFICIENTS FOR THE PRESENTATION OF THE ANGULAR DISTRIBUTIONS

Isotope	^{10}B		^{11}B	
Energy	6 MeV	10 MeV	6 MeV	10 MeV
Elastic (C.M.):				
A_0	73.8	67.2	105.9	69.7
A_1	60.5	104.9	65.6	98.4
A_2	94.9	126.9	138.4	117.7
A_3	84.1	127.1	116.0	126.2
A_4	43.9	79.5	51.2	80.9
A_5	2.2	16.9	3.3	17.3
A_6		15.4		11.6
A_7		6.3		4.6
A_8		5.5		2.3
Nonelastic (lab):				
A_0	13.5	27.3	28.2	41.4
A_1	10.1	13.2	15.6	18.1
A_2	4.6	10.7	6.9	24.6
A_3	2.1	4.2	5.5	12.3
A_4	2.3	6.9	1.2	10.1
A_5	0.9	0.8	3.2	0.6
Total Emission (lab):				
A_0	87.3	94.5	134.1	111.1
A_1	81.6	126.0	95.6	124.9
A_2	104.0	146.3	147.7	149.2
A_3	101.7	150.0	143.2	153.6
A_4	69.8	119.2	84.9	119.9
A_5	20.2	45.3	26.5	43.9
A_6	4.0	23.9	2.1	20.2
A_7	1.0	11.9		9.5
A_8		10.6		6.0
A_9		2.8		

B. *Individual Cross Section Errors*

The final error given with each data point of the secondary neutron spectra consists of the combined counting statistics of the individual spectra plus contributions of various corrections:

- subtraction of white (time-uncorrelated) time-of-flight background
- subtraction of the spectrum of the admixed isotope and other impurities (hydrogen in ^{10}B)
- multiple scattering correction.

For each data point these corrections are uncorrelated and, therefore, their error contributions (see Table XII) were added quadratically. However, within each spectrum these error contributions are correlated (to a degree depending on the type of correction), so that combining uncertainties of individual energy bins quadratically will give a distorted combined error.

To avoid an even stronger masking of the truly random errors, the uncertainty in the neutron detection efficiency which is also strongly correlated is not included. At the secondary neutron energies at which the cross section standard was used (4.0 and 6.7 MeV for the 6- and 10-MeV data, respectively) this uncertainty is even zero. For energies down to about 0.65 MeV the uncertainty can best be expressed[5] by 2%/10 MeV. Below that energy it increases strongly due to the steepness of the efficiency curve and the increasing dependence on the stability of the bias. The uncertainty in the dead-time correction which is less than 0.1% was not folded in either.

TABLE XII

PERCENT EFFECT OF CORRECTIONS ON THE INTEGRATED VALUES OF THE ELASTIC, NONELASTIC, AND TOTAL EMISSION CROSS SECTIONS.

Isotope	^{10}B		^{11}B	
Energy	6 MeV	10 MeV	6 MeV	10 MeV
Hydrogen Contamination (10% [a]):				
elastic	1.6	0.6		
nonelastic	20.8	11.9		
total emission	5.2	3.5		
Monte Carlo Correction[b] (20% [a]):				
elastic	16.3	16.4	8.8	8.3
total emission	15.0	14.3	7.[c]	6.2
Extrapolation of Energy Spectra[c] (50% [a]):				
nonelastic	7 6	3.6	8.4	2.8
total emission	1.2	1.0	1.8	1.0
Extrapolation of Angular Range[d]				
typically 0.5%, up to 1.1%				

a) this fraction of the correction has been added quadratically to the final random errors of the individiual points

b) consisting of multiple scattering, flux attenuation, and geometry corrections

c) correcting for the 0.35-MeV cut-off of the neutron emission spectra

d) effect on A_0 of the Legendre fit when the zero degree value and the 180 degree value are varied within a reasonable range and the number of coefficients used in the fit is changed by one

C. *Scale Uncertainty*

Table XIII compiles the contributions to the scale error. The common scale error is 0.7% and consists of the uncertainty in the number of hydrogen nuclei and in the cross section of the reference sample. The inclusion of the latter into the common scale error is justified by the closeness of the two energies. No substantial systematic error contribution is expected from using polyethelene

instead of hydrogen itself. The close agreement in shape and mass of the polyethylene and the carbon foam samples diminishes background subtraction problems. In addition, the flux depression and multiple scattering in both samples were corrected for by Monte Carlo calculation.

The other contributions listed in Table XIII except for the last one are identical either for the two energies or the two samples. Neglecting the correlations, the combined scale errors of the four measurements are between 1.9% and 2.2%.

D. *Uncertainties of Integrated Data*

The uncertainties given in Tables IX and X were obtained by adding quadratically the individual errors disregarding any correlation. To provide more information on possible correlations, Table XII lists the effect of the corrections on the integrated data together with the percentage which was used for the quadratic addition to the random error of the individual points. More details are given in the footnotes of the table.

VI. DISCUSSION

Except for data near 14 MeV[10,11] no previous data on neutron emission spectra for these targets are known. Only scattering from elastic and some inelastic levels has been reported in the energy range covered in this experiment: Glendinning et al.[12] from 8 to 14 MeV, Cookson and Locke[13] at 9.72 MeV, and White et al.[14] and Knox et al.[15], respectively, below 8 MeV. The present data at 10 MeV are generally lower by 5 to 10% than previous data[12,13]. The agreement in the shape is moderate to poor except for ^{11}B.

There, an astoundingly good agreement in shape is found with the data of Glendinning et al.[12] when a difference in the 0^{o} direction of 0.7^{o} is taken into account.

TABLE XIII

CONTRIBUTIONS TO THE SCALE ERROR

1.	**Energy Independent Contributions:**	^{10}B		^{11}B
1.1	Standard			
	mass (weight, purity)		<0.5%	
	cross section [a]		<0.5%	
1.2	Sample			
	mass (weight, purity)	<1%		<1%
2.	**Energy Dependent Contributions:**	6 MeV		10 MeV
2.1	Standard			
	peak evaluation [b]	0.5%		0.9%
	normalization [c]	<0.5%		<0.5%
	Monte Carlo correction [d]	0.7%		1.1%
	geometry [e]	1.0%		1.0%
2.2	Samples			
	Monte Carlo correction [f]			

a) uncertainty in the $^{1}H(n,n)^{1}H$ reference cross section at 6 and 10 MeV is expected to be so strongly correlated that it can be assumed to be "energy independent"

b) consists of the combined statistical errors, the error in the dead-time correction and in the background subtraction

c) calibration of the experimental set-up using a detector with a given efficiency curve in a given geometry; it depends on the evaluation of the monitor counts and the beam charge collection

d) the Monte Carlo simulation corrects for flux attenuation, multiple scattering, and finite sample size

e) difference in the positioning of the sample with regard to the neutron source and the detector; within one angular distribution this uncertainty is uncorrelated, but not for the reference measurement

f) uncertainties connected with the flux depression in the sample are clearly correlated within each angular distribution; in the present case this systematic error contribution was not extracted from the total uncertainty of this correction

Table XIV compares the integrated cross sections with the values of ENDF/B-V and some recent total cross section measurements[9]. At these lower energies the total cross sections of ^{11}B are also too low in ENDF/B-V, analogous to our findings[3] at 14 MeV.

A comparison with the data of Auchampaugh et al.[9] gives a very good agreement for ^{11}B where there is no or only little difference between the integrated total emission cross section and the total cross section. However, for ^{10}B it suggests that the present ^{10}B data are low by about 2.8% if the charged particle data taken from ENDF/B-V are correct. This difference itself is only slightly outside the combined scale errors. However, the ratio between the ^{10}B and ^{11}B cross sections is much more accurate because of the strong correlation in the scale errors (see Table XIII) so that there appears to be a systematic discrepency.

On the other hand, a comparison of the integrated elastic cross sections at 10 MeV with those of Glendinning et al.[12] suggests that the scale of our ^{10}B data is high compared to that of ^{11}B. Also, the very good agreement of the integrated total emission data of ^{10}B with the values given in ENDF/B-V further supports our present solution. Thus, the (small) difference between our data and those of Auchampaugh et al.[9] is supported by other data. Possible causes for it are either the non-neutron cross sections involved or the insufficient quality of the data bases for the Monte Carlo simulation.

TABLE XIV

COMPARISON OF INTEGRATED CROSS SECTIONS *(in barns)*

Energy (MeV)	Sample	Elastic exp[a]	Elastic eval[b]	Total Emission exp[a]	Total Emission eval[b]	Total Reaction exp[a]	Total Reaction Ref.9
6.00	^{10}B	0.898[c]	0.951	1.097	1.096	1.50[d]	1.54
10.00	^{10}B	0.834[c]	0.931	1.187	1.196	1.44[d]	1.49
6.00	^{11}B	1.331	1.426	1.685	1.555	1.69	1.66
10.00	^{11}B	0.876	0.886	1.396	1.274	1.41[d]	1.41

a) this work

b) ENDF/B-V

c) cross section of unresolved excited states subtracted

d) uses ENDF/B-V values for non-neutron reactions

REFERENCES

1. D. M. Drake, G. F. Auchampaugh, E. D. Arthur, C. E. Ragan, and P. G. Young, Nucl. Sci. Eng. 63, 401 (1977).

2. P. W. Lisowski, G. F. Auchampaugh, D. M. Drake, M. Drosg, G. Haouat, N. W. Hill, and L. Nilsson, "Cross Sections For Neutron-Induced, Neutron-Producing Reactions In ^{6}Li and ^{7}Li At 5.96 And 9.83 MeV," Los Alamos Scientific Laboratory report LA-8342-MS (1980).

3. M. Drosg, P. W. Lisowski, D. M. Drake, R. A. Hardekopf, and M. Muellner,"Cross Sections For Neutron-Producing Reactions Induced By 14.1 MeV Neutrons in ^{6}Li, ^{7}Li, ^{10}B, ^{11}B, and Carbon," (in preparation).

4. J. C. Hopkins and G. Breit, Nucl. Data Tables A9, 137 (1971).

5. M. Drosg, D. M. Drake, and P. Lisowski, Nucl. Instr. Methods 176, 477 (1980).

6. Los Alamos Scientific Laboratory Group X-6, "MCNP - A General Monte Carlo Code for Neutron and Photon Transport," Los Alamos Scientific Laboratory report LA-7396-M, Rev. (November 1979).

7. F. Ajzenberg-Selove, Nucl. Phys. A413, 1 (1984).

8. F. Ajzenberg-Selove, Nucl. Phys. A433, 1 (1985).

9. G. F. Auchampaugh, C. E. Ragan, S. Plattard, and N. W. Hill, "Neutron Total Cross-Section Measurements of ^{9}Be, ^{10,11}B, and ^{12,13}C from 1.0 to 14 MeV using the ^{9}Be(d,n)^{10}B Reaction as a "White" Neutron Source," Los Alamos Scientific Laboratory report LA-6761-MS (1977).

10. S. C. Mathur, P. S. Buchanan, and L. L. Morgan, Phys. Rev. 186, 1038 (1969).

11. M. Baba, M. Ono, N. Yabuta, T. Kikuti, and N. Hirakawa, "Scattering of 14.1-MeV Neutrons from ^{10}B, ^{11}B, C, N, O, F and Si," Radiation Effects, to be published.

12. S. G. Glendinning, S. El-Kadi, C. E. Nelson, R. S. Pedroni, F. O. Purser, R. L. Walter, A. G. Beyerle, C. R. Gould, L. W. Seagondollar, and P. Thambidurai, Nucl. Sci. Eng. 80, 256 (1982).

13. J. A. Cookson and J. G. Locke, Nucl. Phys. A146, 417 (1970).

14. R. M. White, R. O. Lane, and H. D. Knox, Nucl. Phys. A340, 13 (1980).

15. H. D. Knox, R. M. White, and R. O. Lane, Nucl. Sci. Eng. 65, 65 (1978).

APPENDIX

SPECTRA OF THE UNCORRECTED DOUBLE DIFFERENTIAL LABORATORY CROSS SECTIONS FOR ^{10}B AND ^{11}B AT 6 AND 10 MEV FOR ANGLES BETWEEN 20^{o} AND 145^{o}

In Figs. A-1 through A-38, the full curves are the experimental results, the dotted curves are the straight answer of a Monte Carlo simulation using ENDF/B-IV input data and the dashed curves are the piecewise adjusted curves used in this paper for determining the multiple scattering correction.

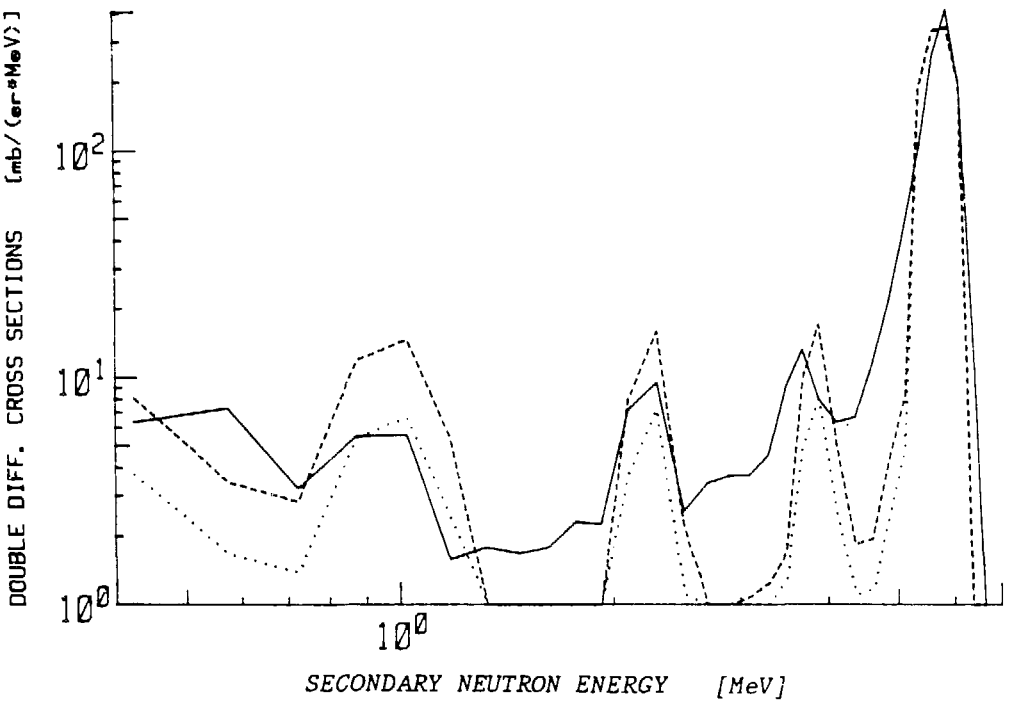

Fig. A-1. 6.0 MeV Neutrons on Boron-10 20.0 Deg.

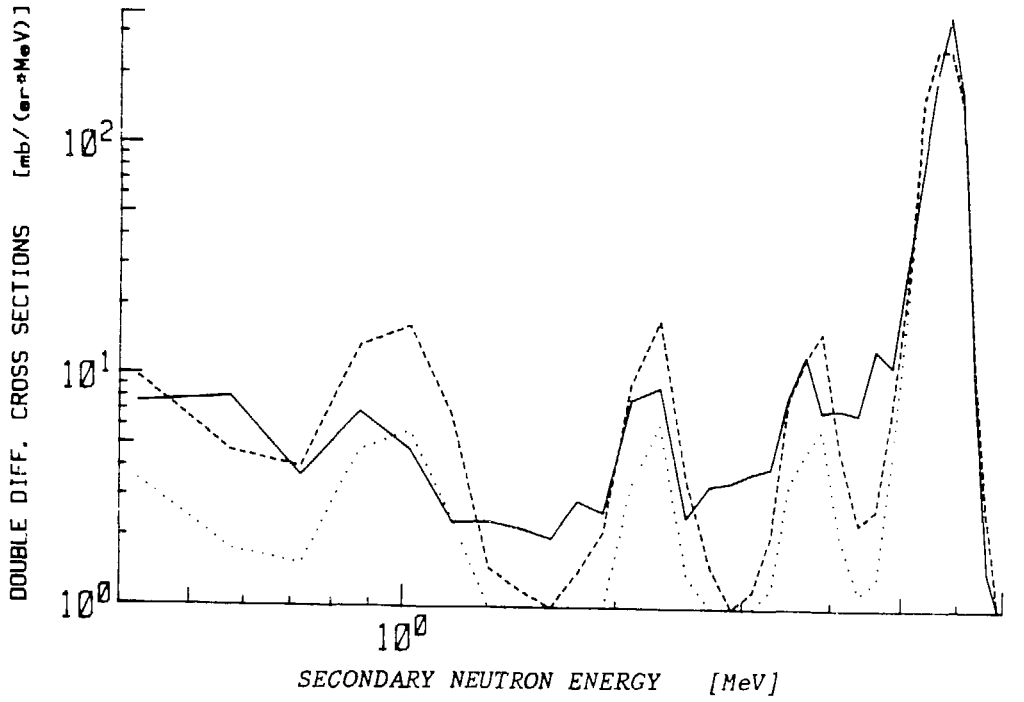

Fig. A-2. 6.0 MeV Neutrons on Boron-10 25.0 Deg.

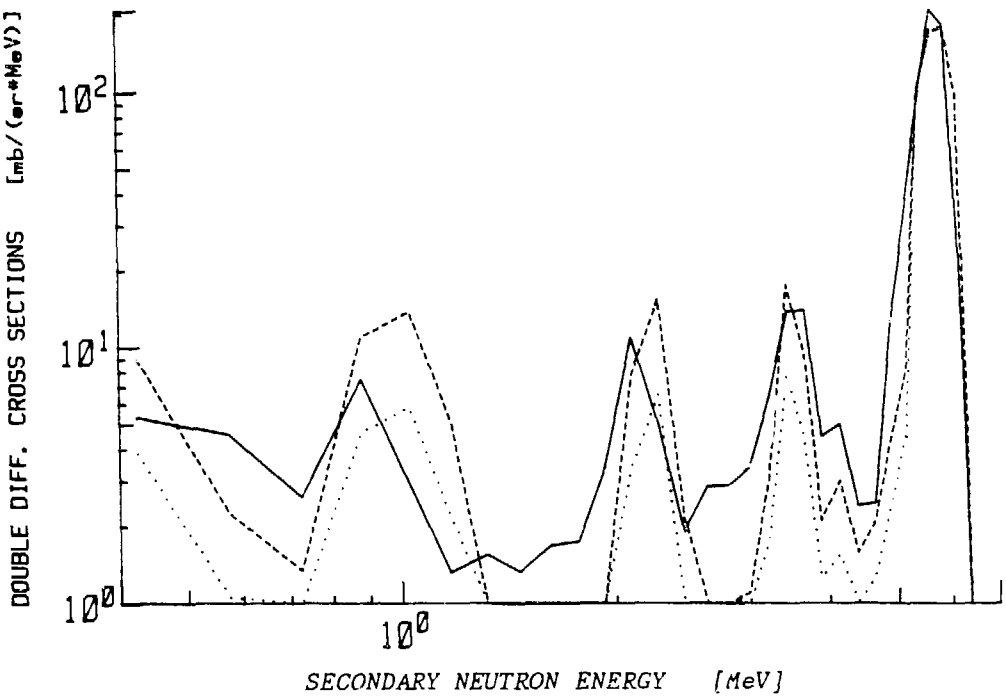

Fig. A-3. 6.0 MeV Neutrons on Boron-10 35.0 Deg.

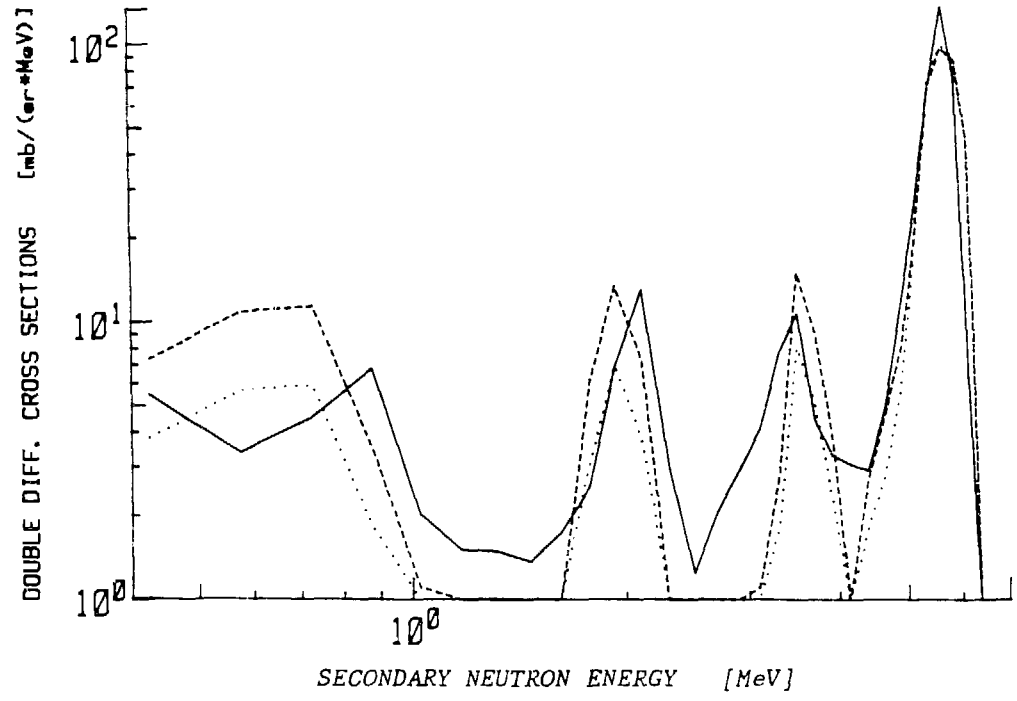

Fig. A-4. 6.0 MeV Neutrons on Boron-10 45.0 Deg.

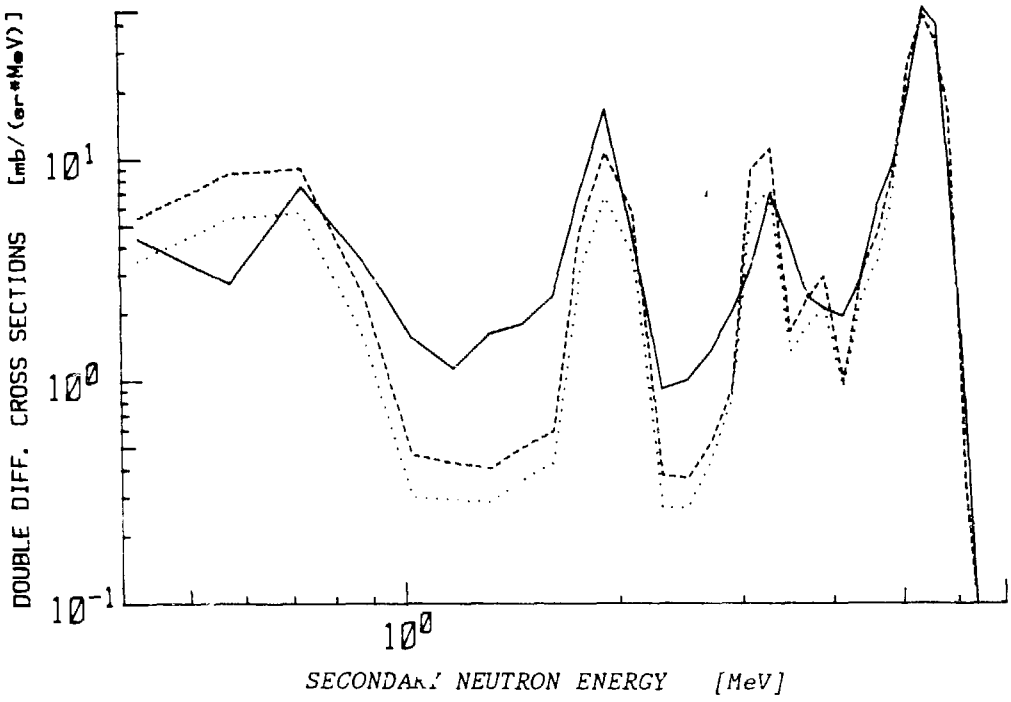

Fig. A-5. 6.0 MeV Neutrons on Boron-10 60.0 Deg.

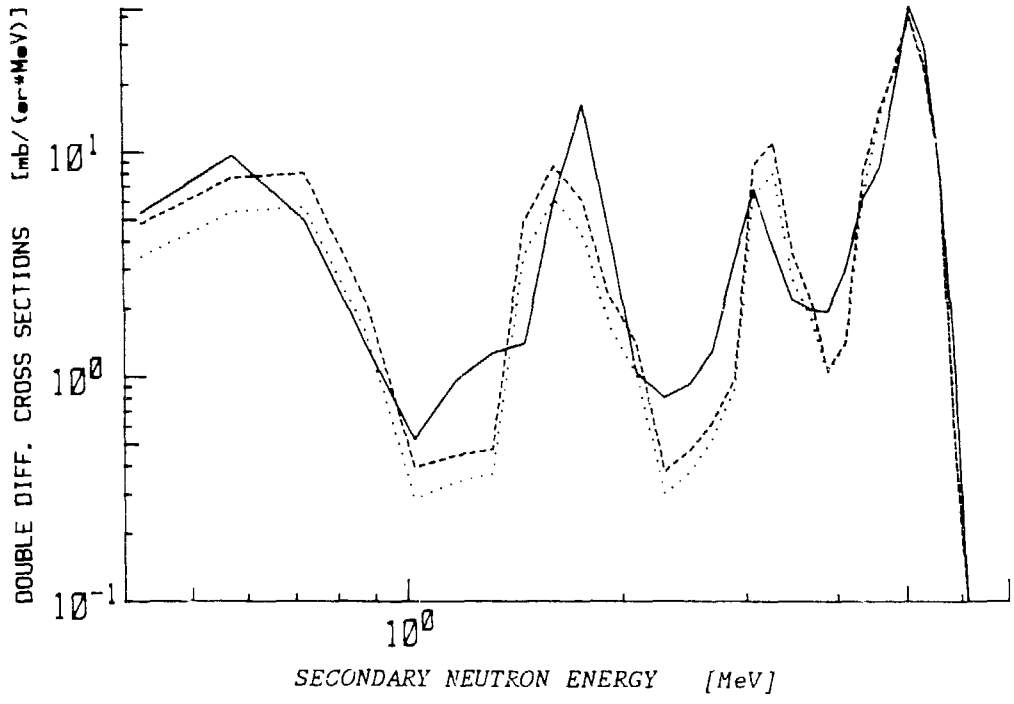

Fig. A-6. 6.0 MeV Neutrons on Boron-10 75.0 Deg.

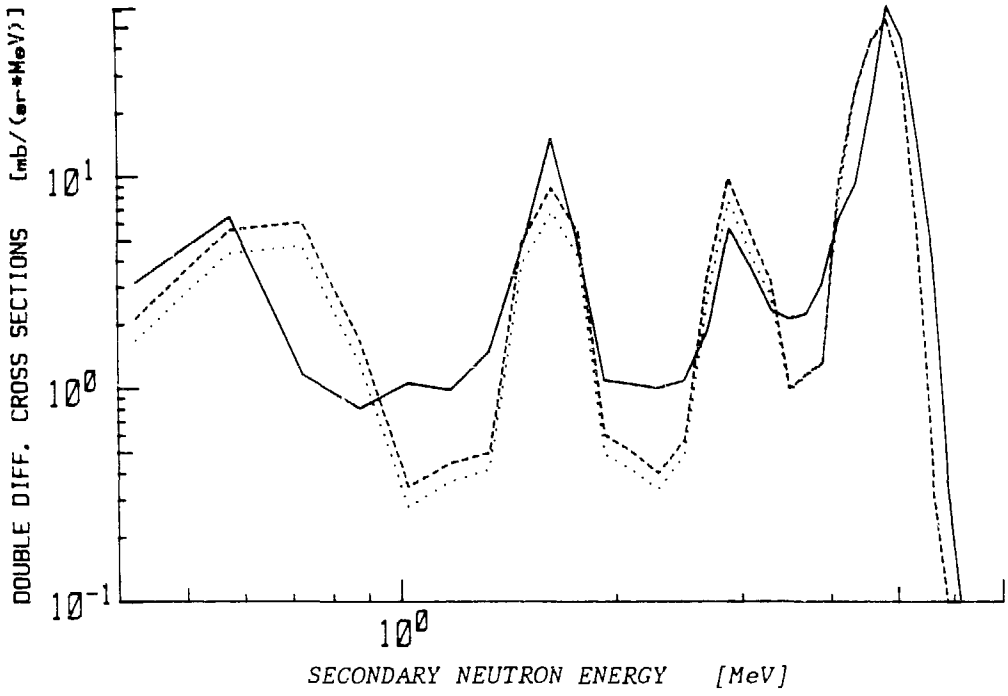

Fig. A-7. 6.0 MeV Neutrons on Boron-10 90.0 Deg.

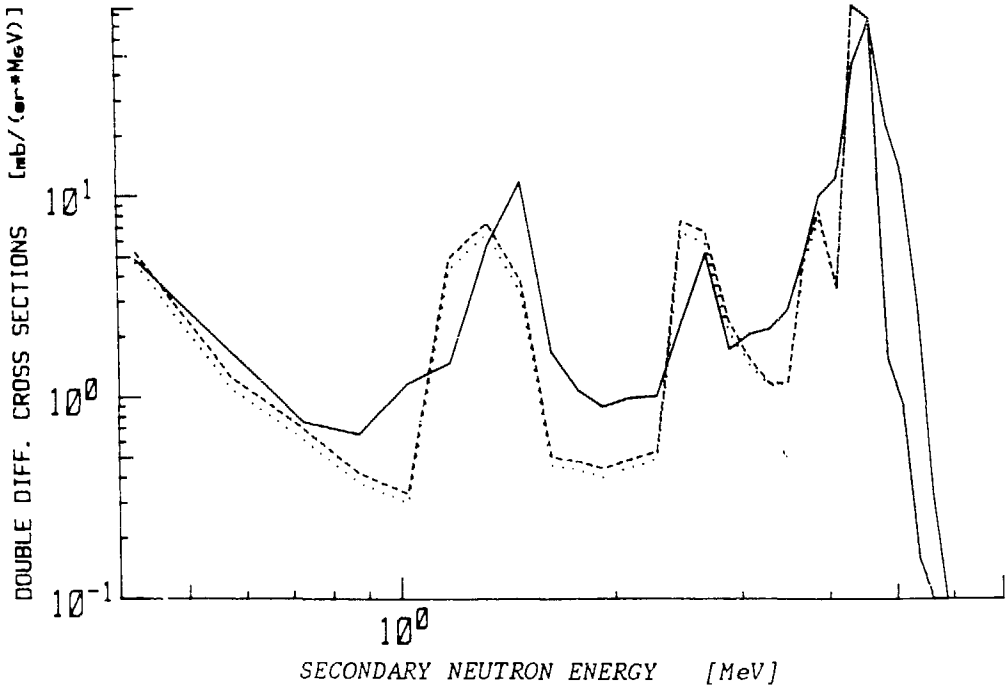

Fig. A-8. 6.0 MeV Neutrons on Boron-10 110.0 Deg.

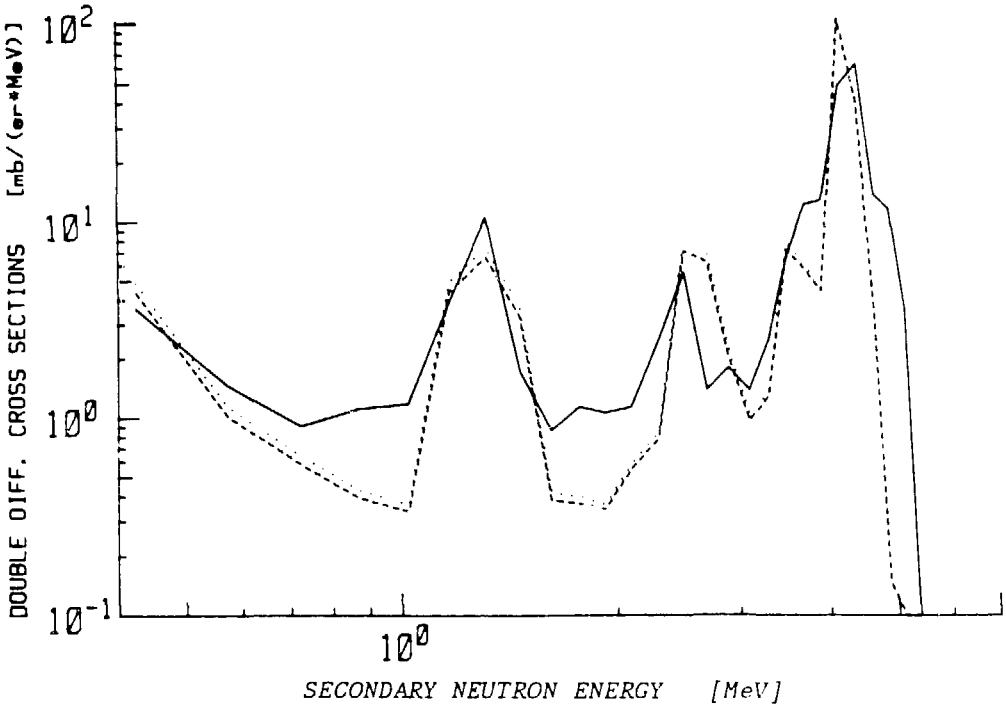

Fig. A-9. 6.0 MeV Neutrons on Boron-10 130.0 Deg.

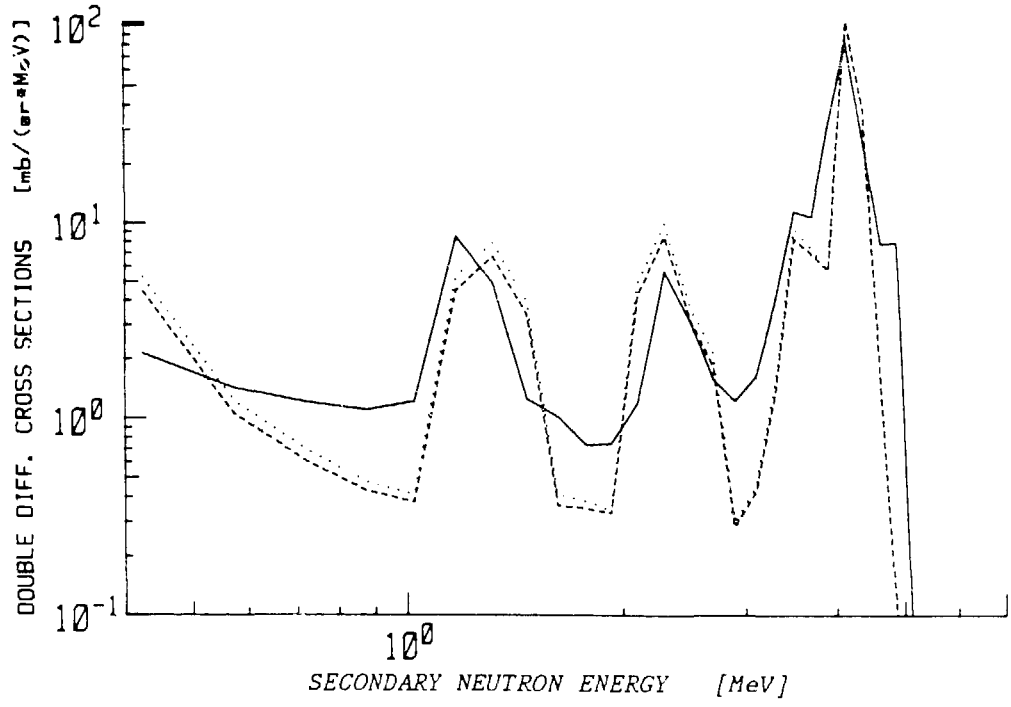

Fig. A-10. 6.0 MeV Neutrons on Boron-10 145.0 Deg.

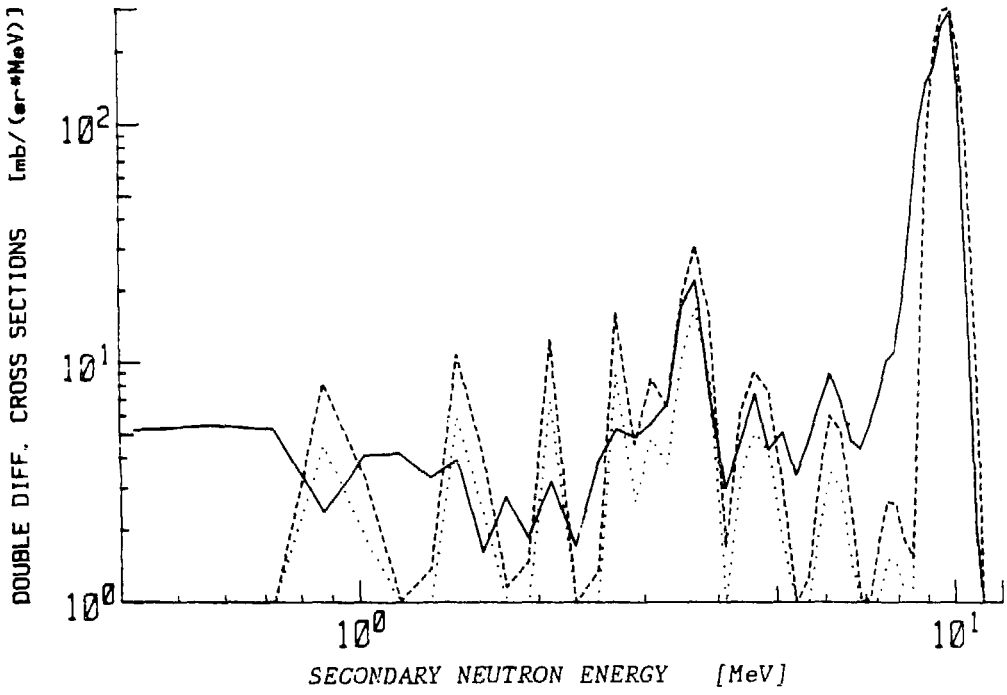

Fig. A-11. 10.0 MeV Neutrons on Boron-10 20.0 Deg.

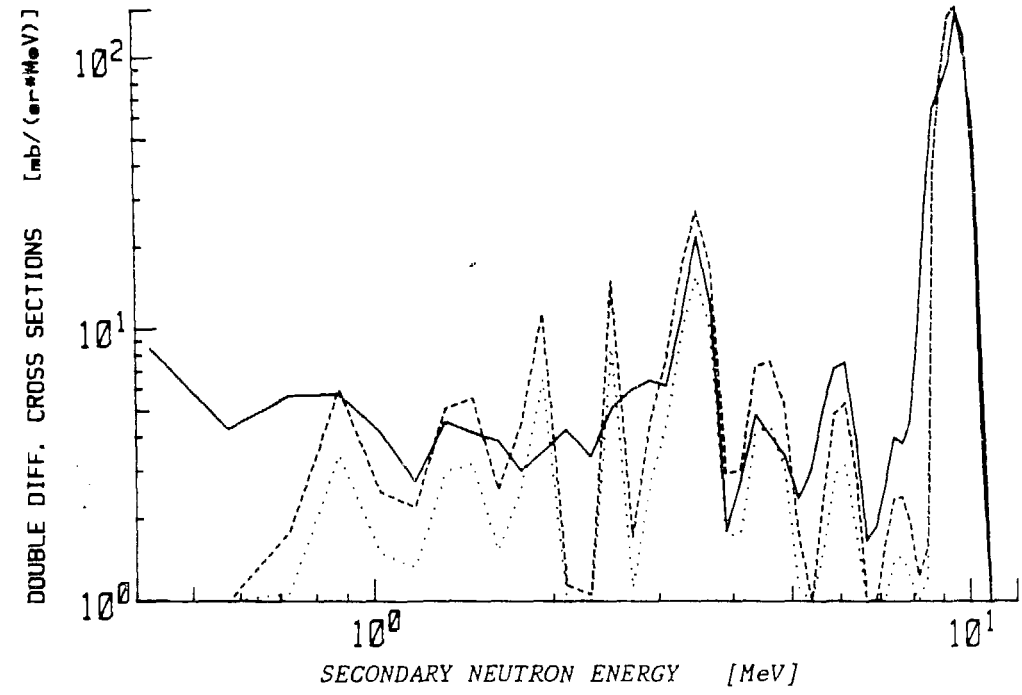

Fig. A-12. 10.0 MeV Neutrons on Boron-10 35.0 Deg.

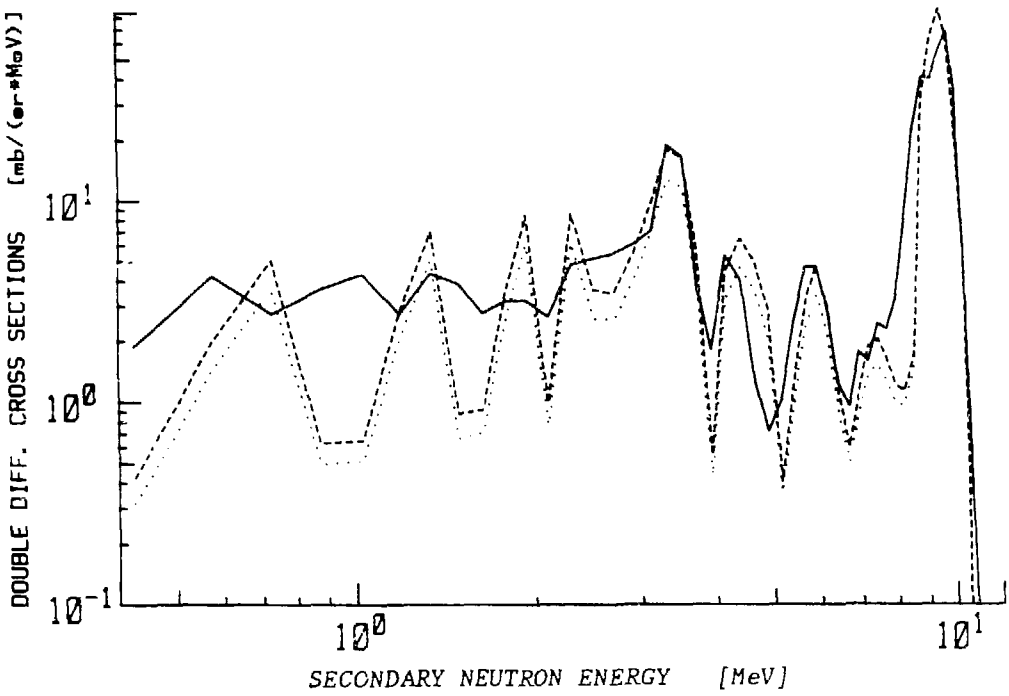

Fig. A-13. 10.0 MeV Neutrons on Boron-10 45.0 Deg.

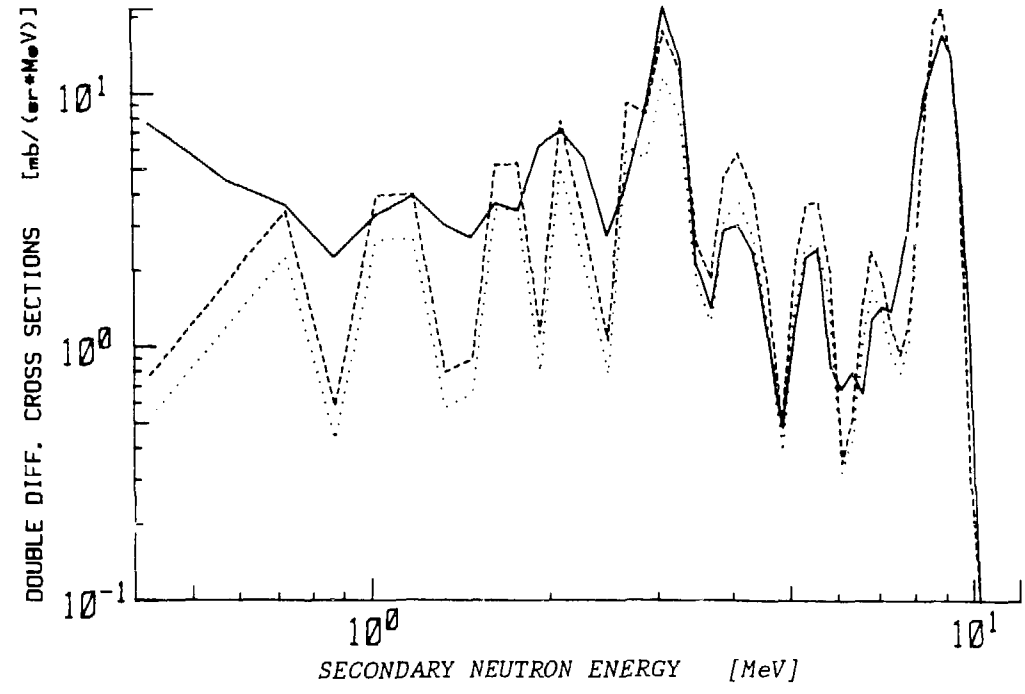

Fig. A-14. 10.0 MeV Neutrons on Boron-10 60.0 Deg.

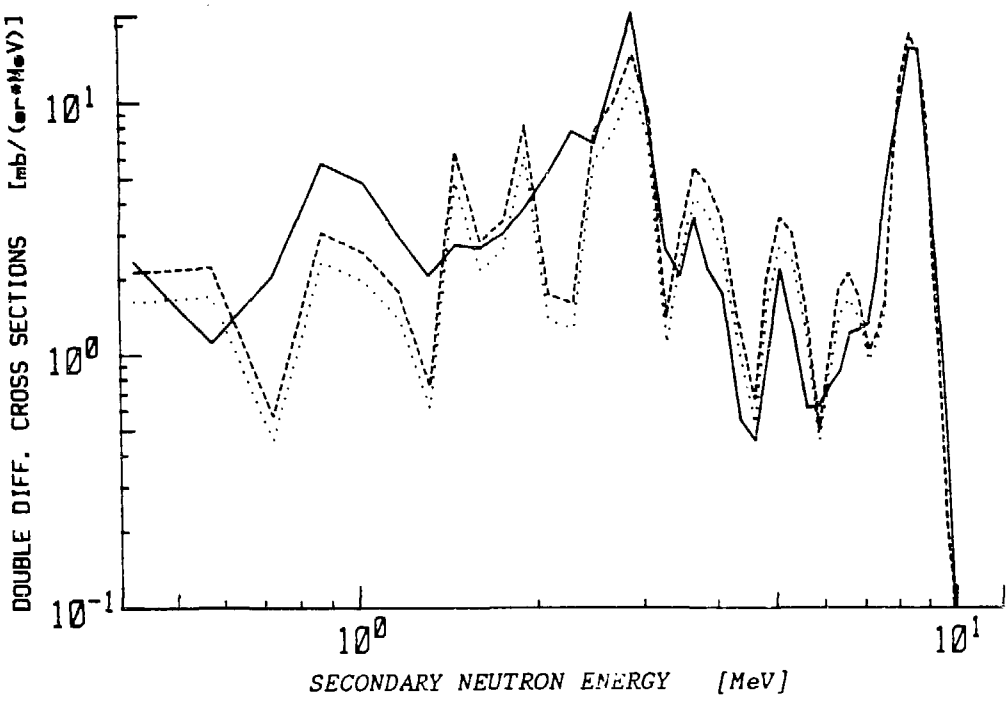

Fig. A-15. 10.0 MeV Neutrons on Boron-10 75.0 Deg.

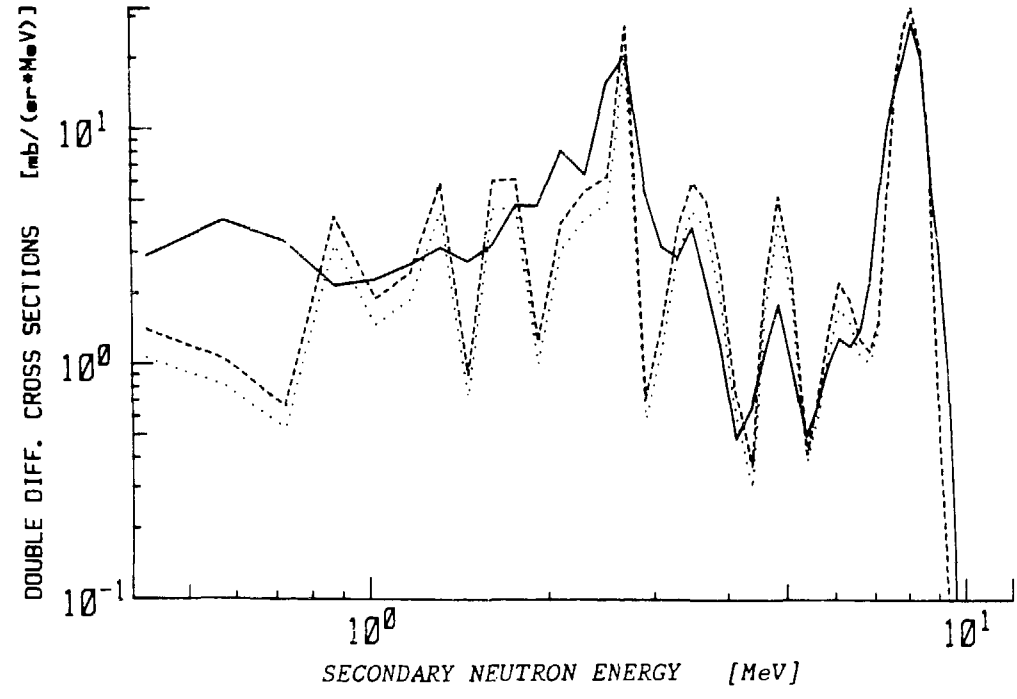

Fig. A-16. 10.0 MeV Neutrons on Boron-10 90.0 Deg.

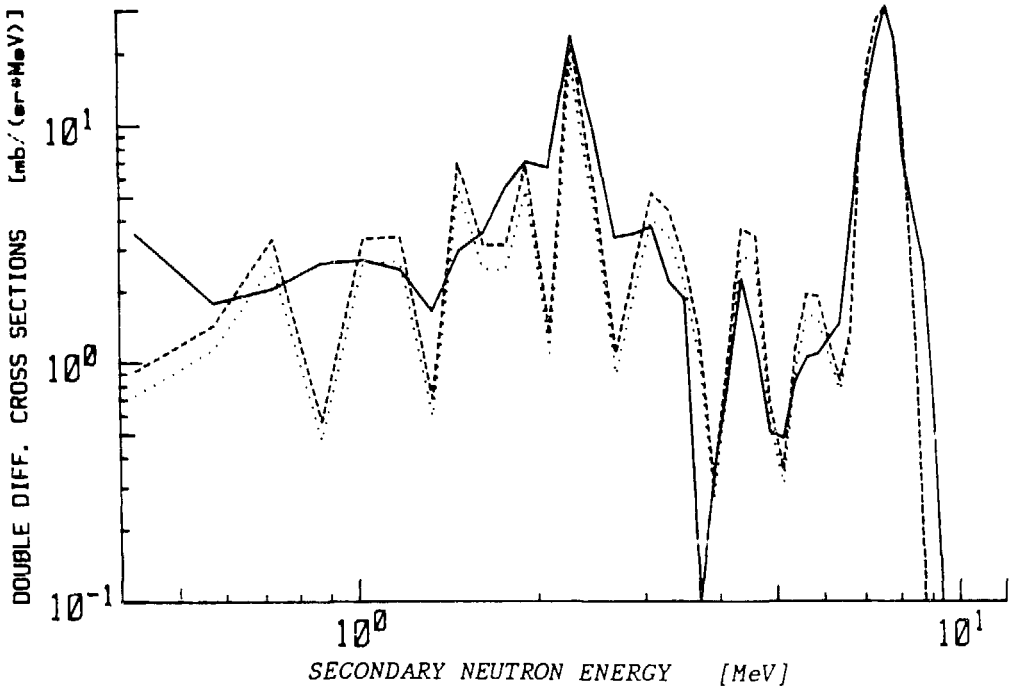

Fig. A-17. 10 MeV Neutrons on Boron-10 110.0 Deg.

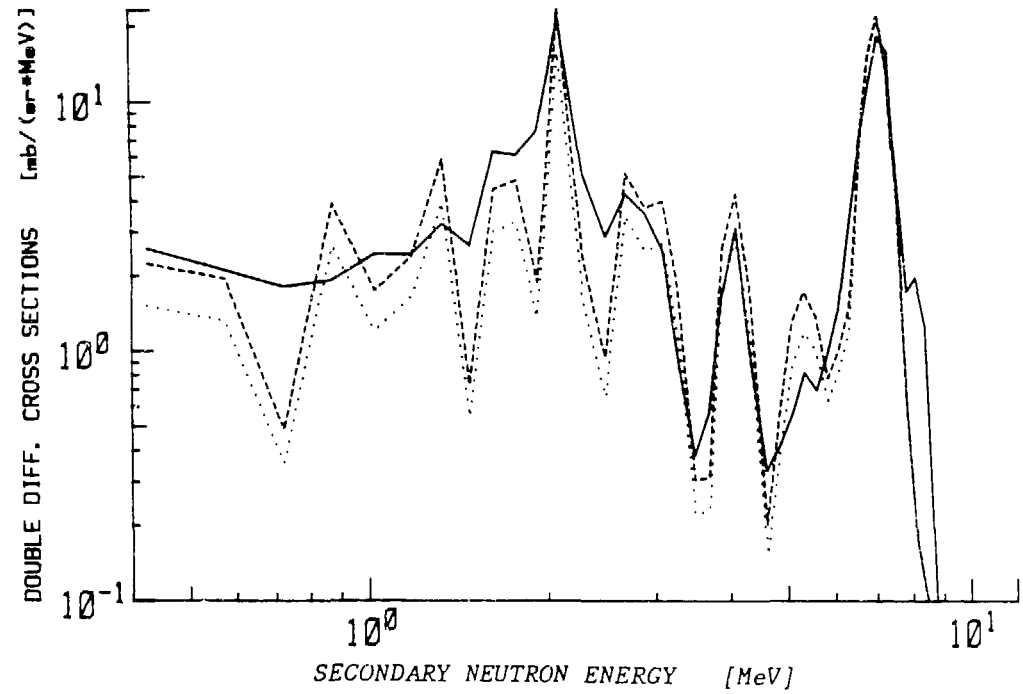

Fig. A-18. 10.0 MeV Neutrons on Boron-10 130.0 Deg.

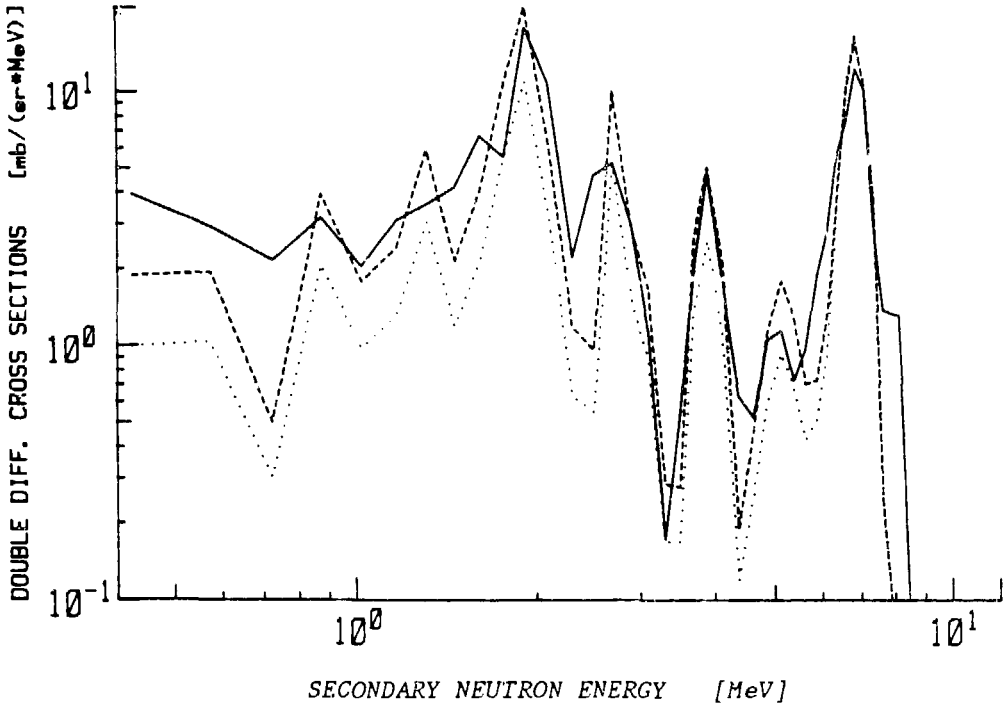

Fig. A-19. 10.0 MeV Neutrons on Boron-10 145.0 Deg.

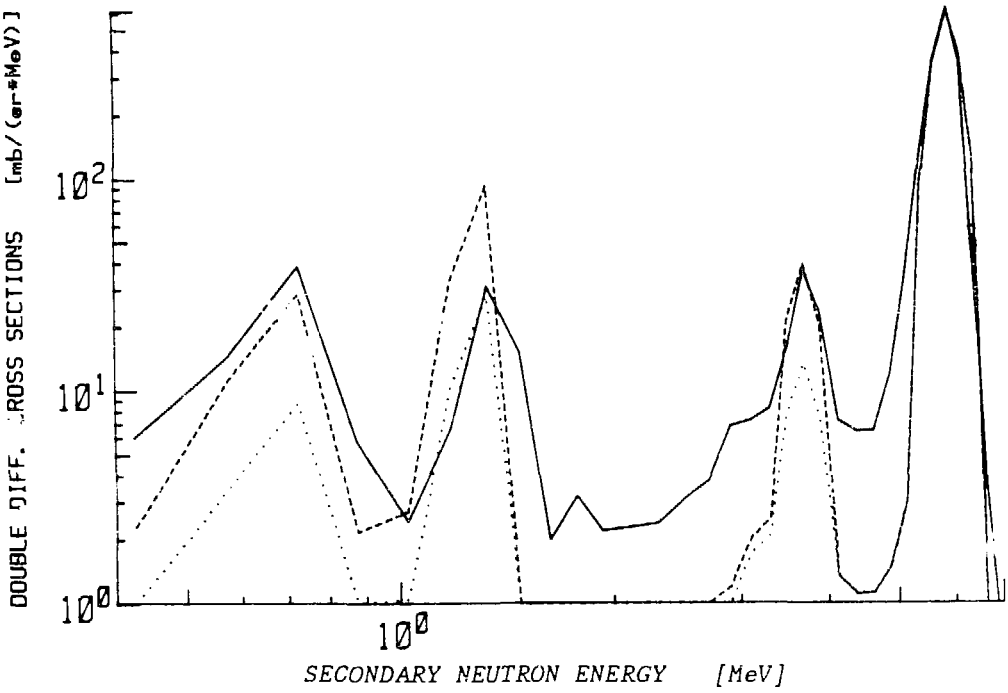

Fig. A-20. 6.0 MeV Neutrons on Boron-11 20.0 Deg.

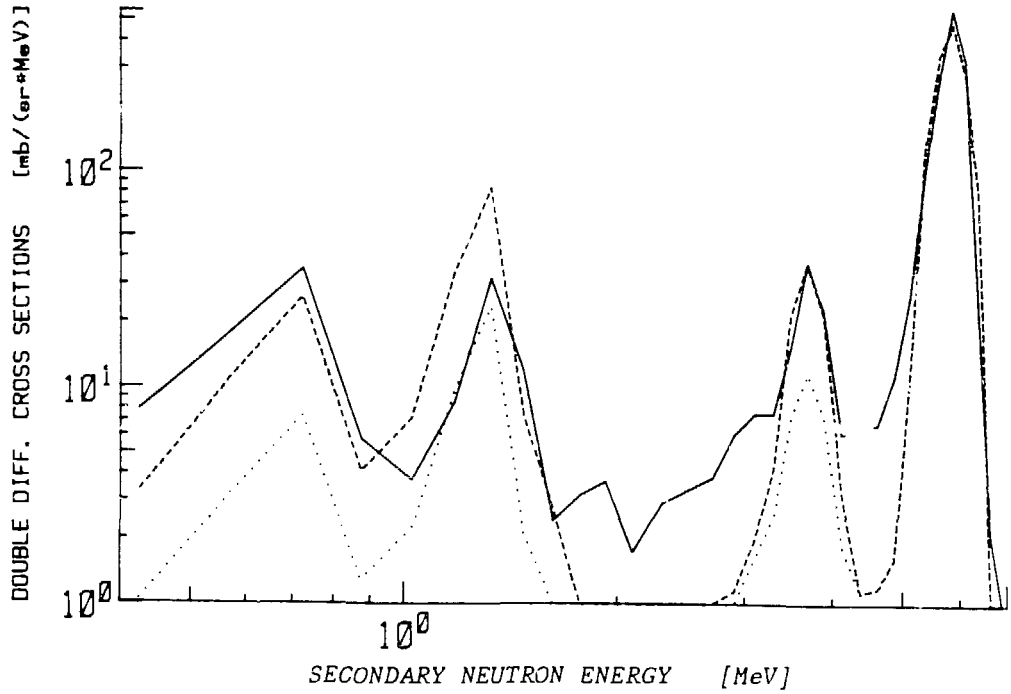

Fig. A-21. 6.0 MeV Neutrons on Boron-11 25.0 Deg.

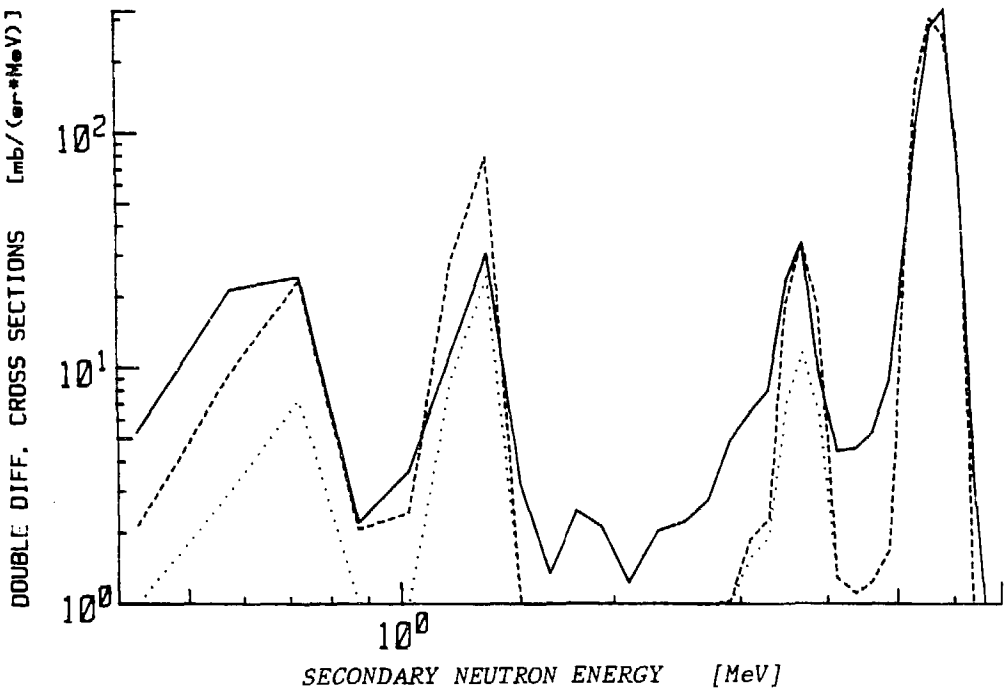

Fig. A-22. 6.0 MeV Neutrons on Boron-11 35.0 Deg.

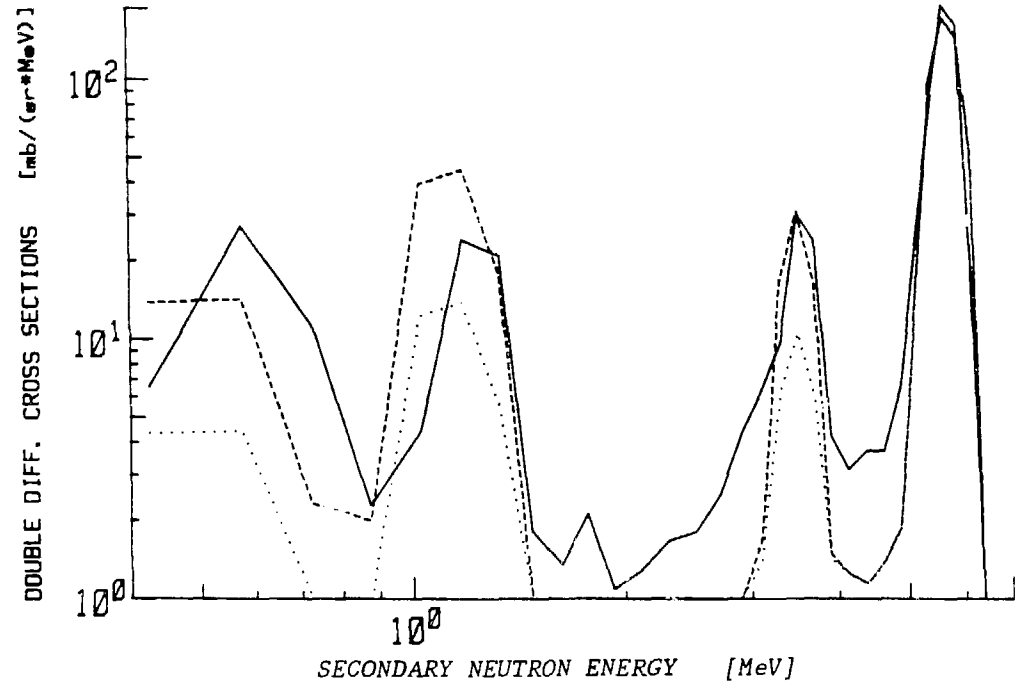

Fig. A-23. 6.0 MeV Neutrons on Boron-11 45.0 Deg.

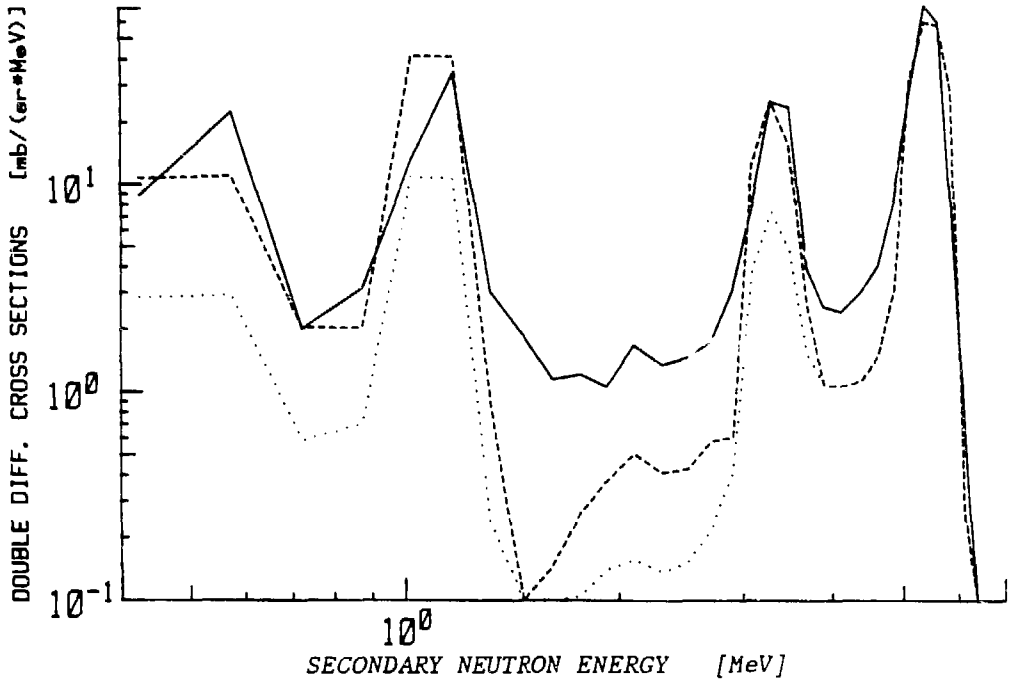

Fig. A-24. 6.0 MeV Neutrons on Boron-11 60.0 Deg.

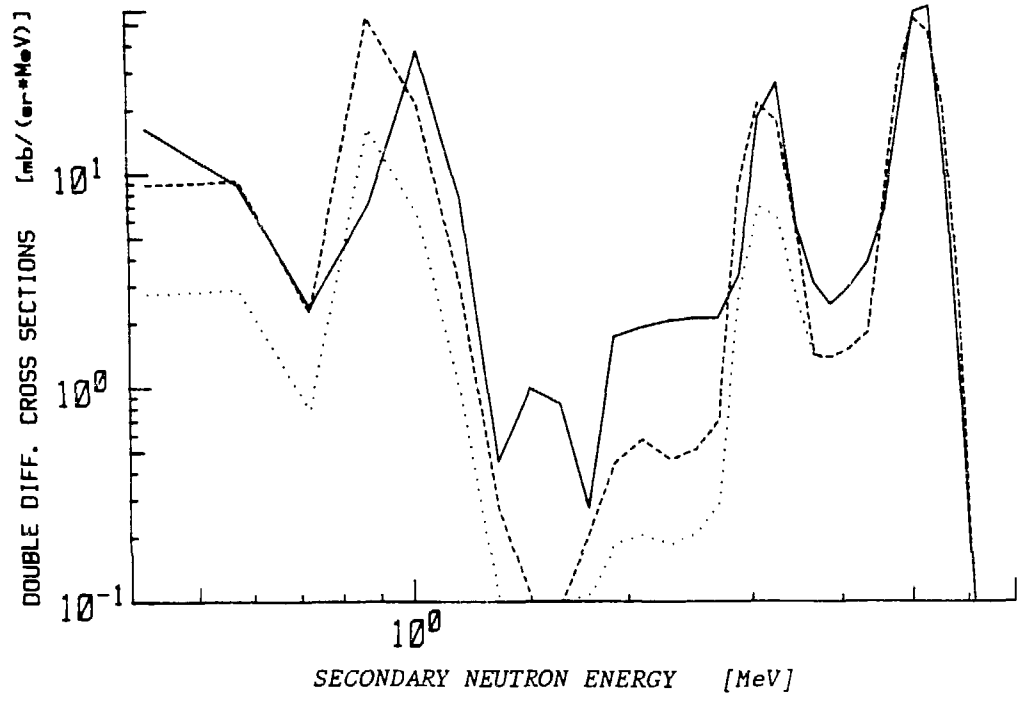

Fig. A-25. 6.0 MeV Neutrons on Boron-11 75.0 Deg.

Fig. A-26. 6.0 MeV Neutrons on Boron-11 90.0 Deg.

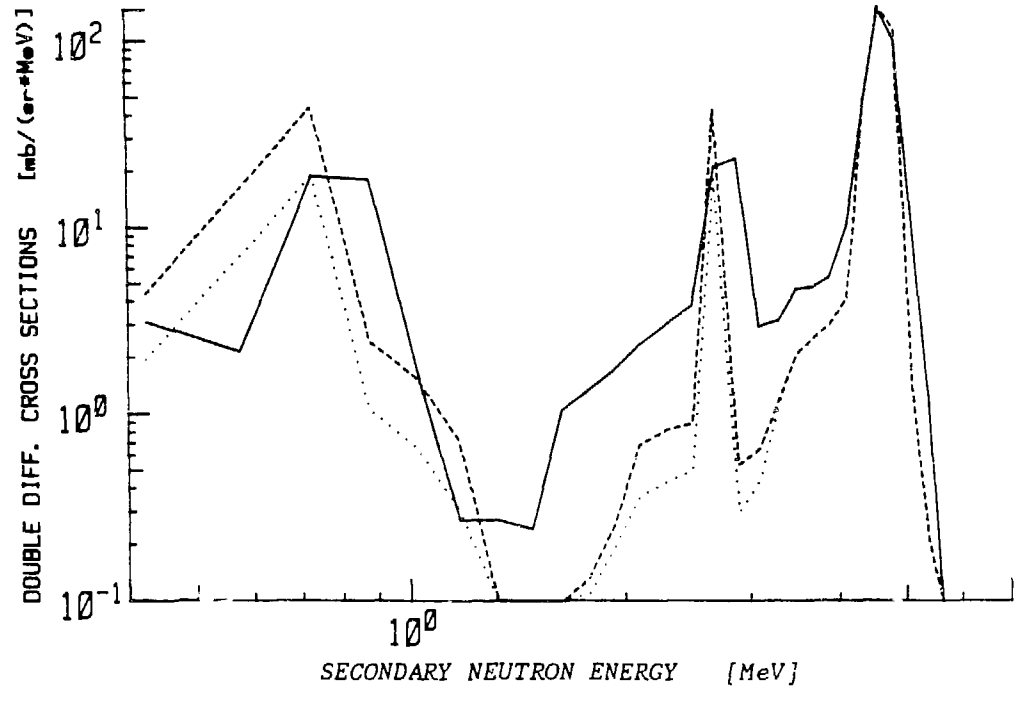

Fig. A-27. 6.0 MeV Neutrons on Boron-11 110.0 Deg.

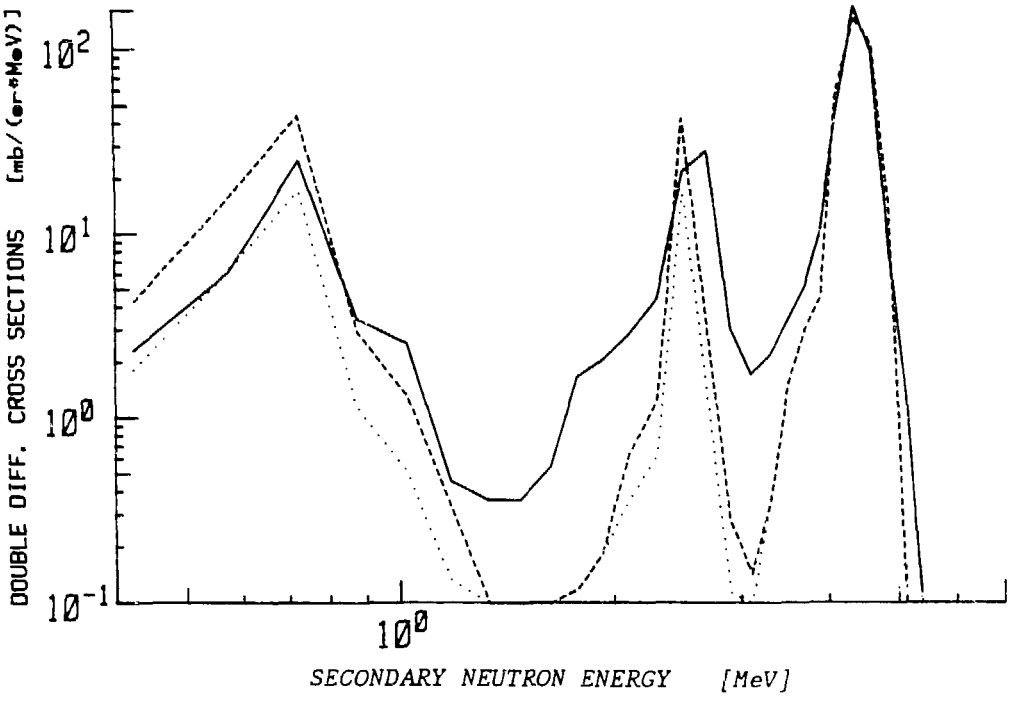

Fig. A-28. 6.0 MeV Neutrons on Boron-11 130.0 Deg.

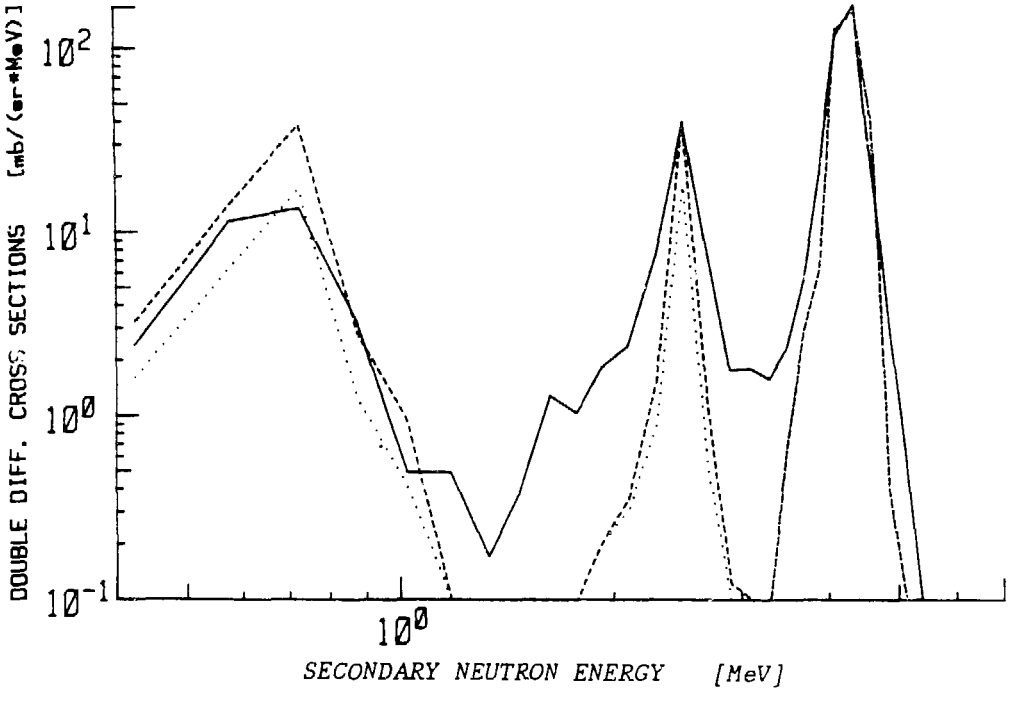

Fig. A-29. 6.0 MeV Neutrons on Boron-11 145.0 Deg.

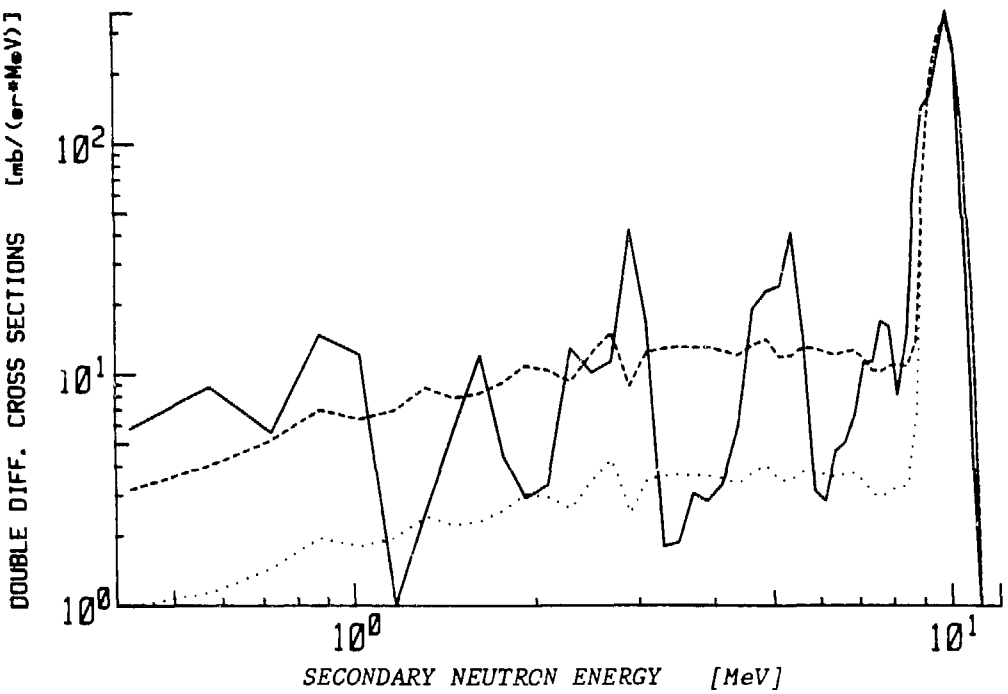

Fig. A-30. 10.0 MeV Neutrons on Boron-11 20.0 Deg.

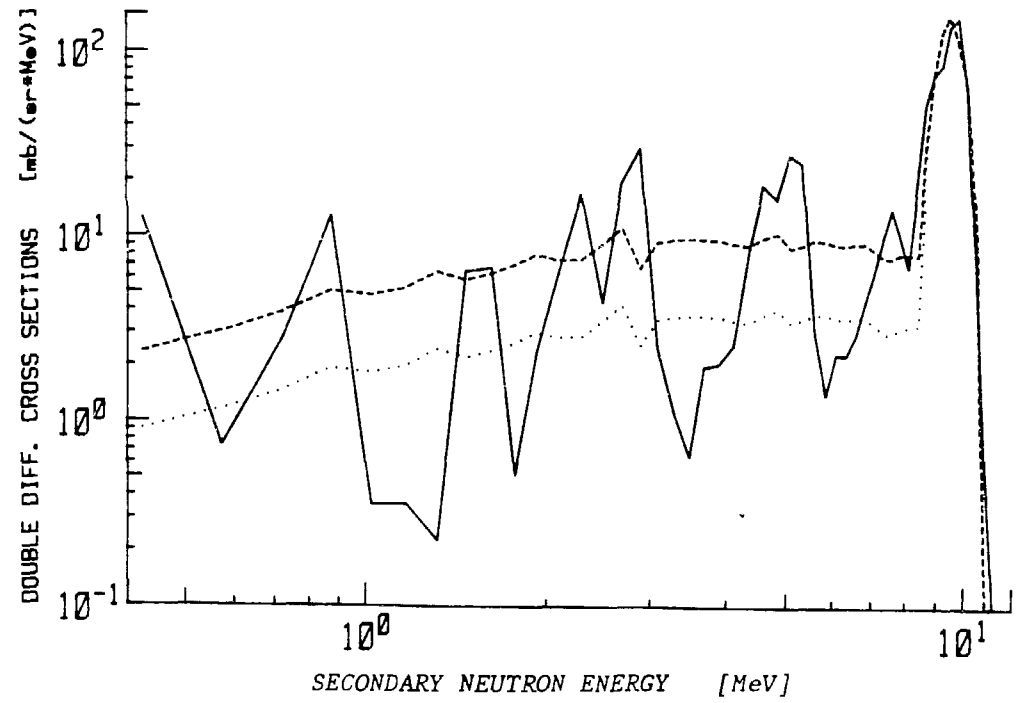

Fig. A-31. 10.0 MeV Neutrons on Boron-11 35.0 Deg.

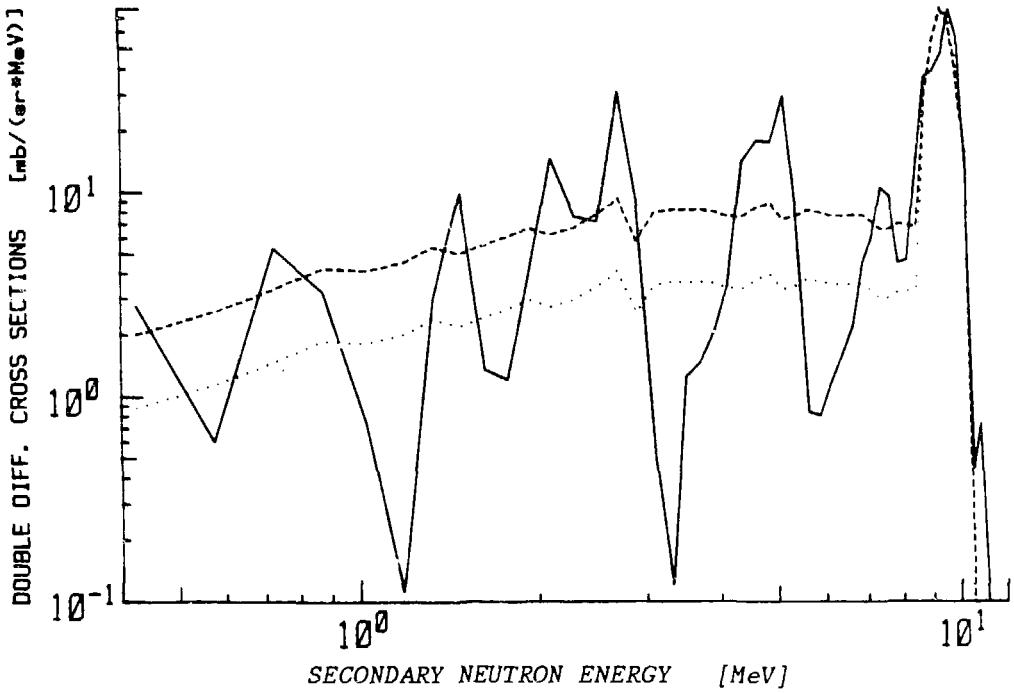

Fig. A-32. 10.0 MeV Neutrons on Boron-11 45.0 Deg.

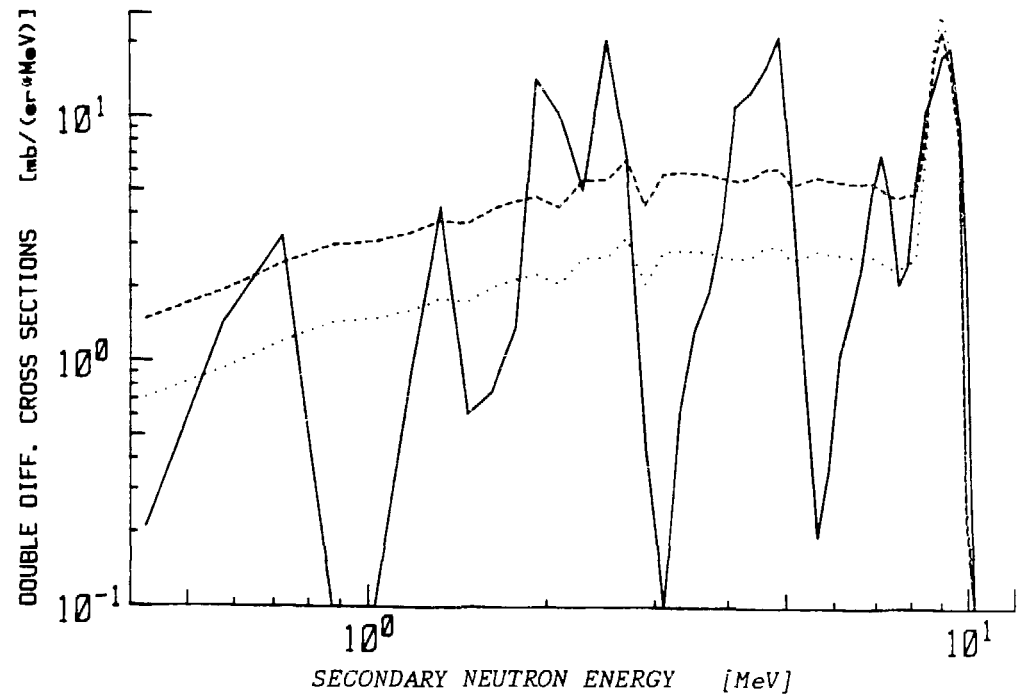

Fig. A-33. 10.0 MeV Neutrons on Boron-11 60.0 Deg.

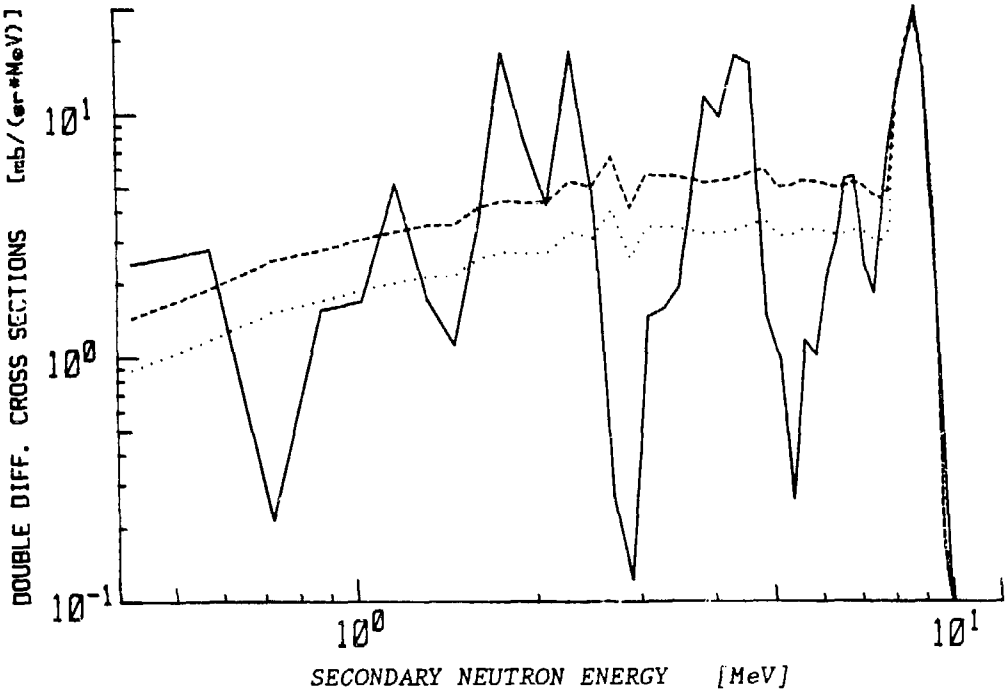

Fig. A-34 10.0 MeV Neutrons on Boron-11 75.0 Deg.

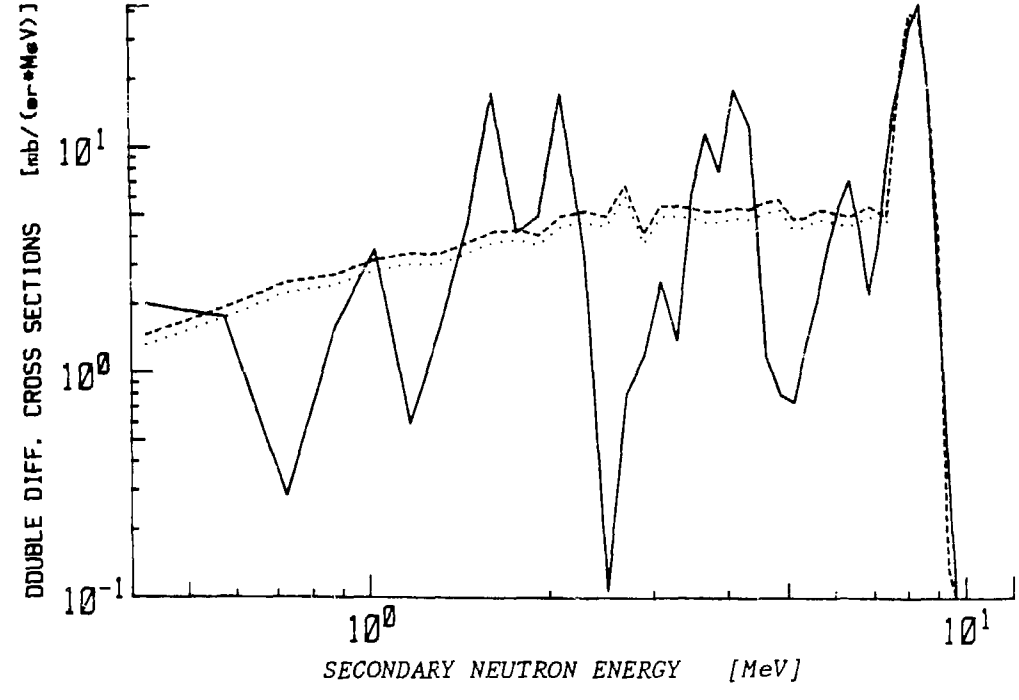

Fig. A-35. 10.0 MeV Neutrons on Boron-11 90.0 Deg.

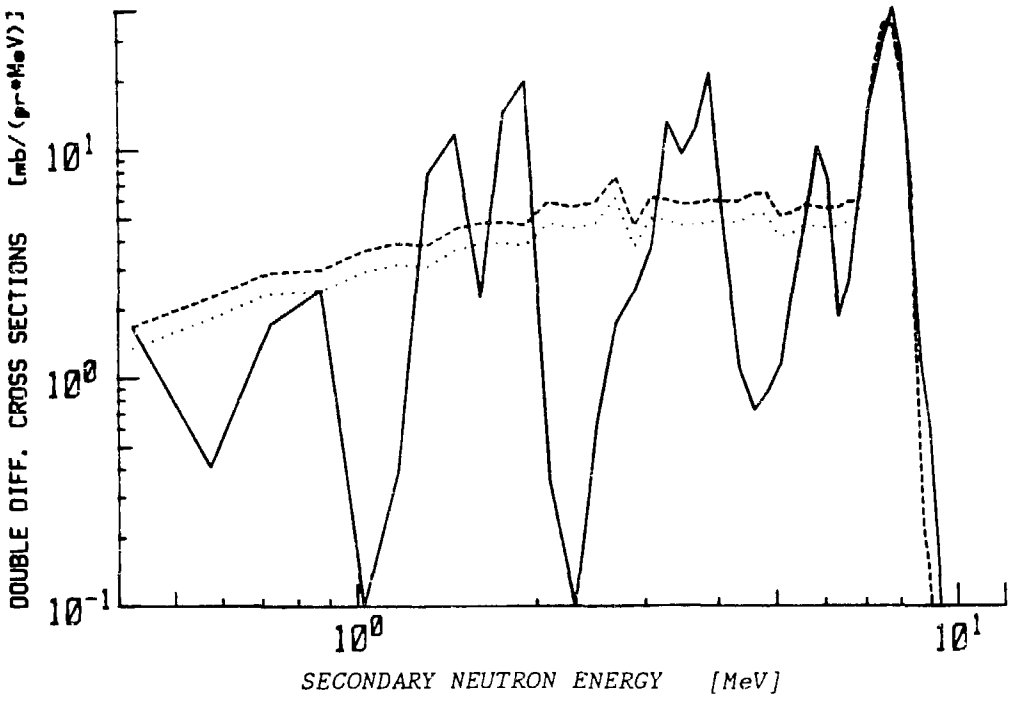

Fig. A-36. 10.0 MeV Neutrons on Boron-11 110.0 Deg.

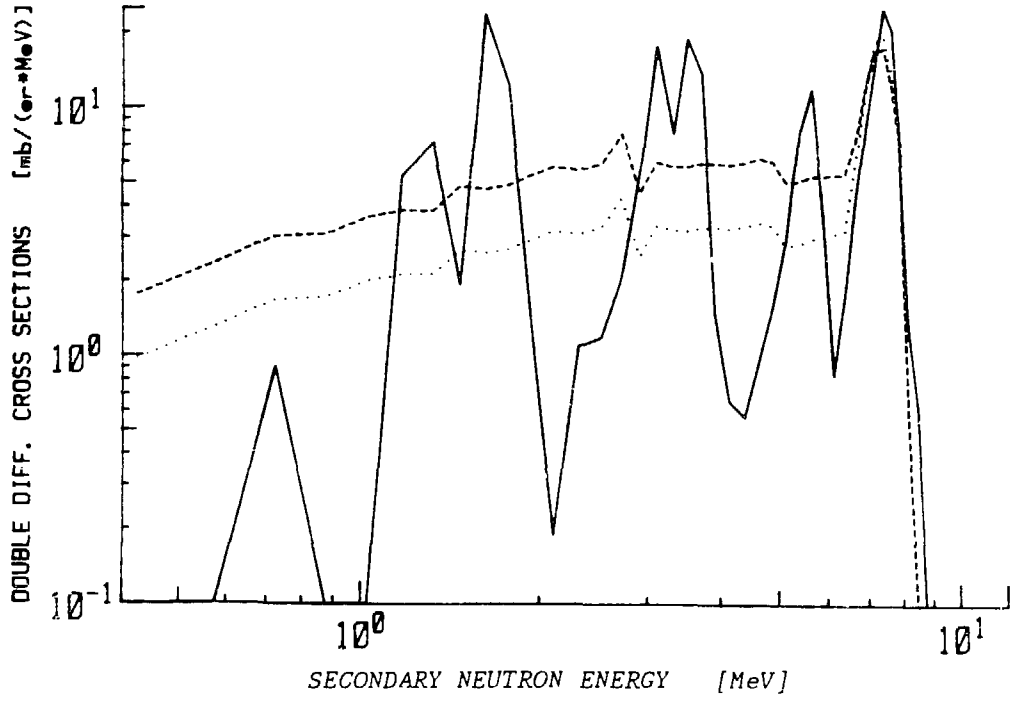

Fig. A-37. 10.0 MeV Neutrons on Boron-11 130.0 Deg.

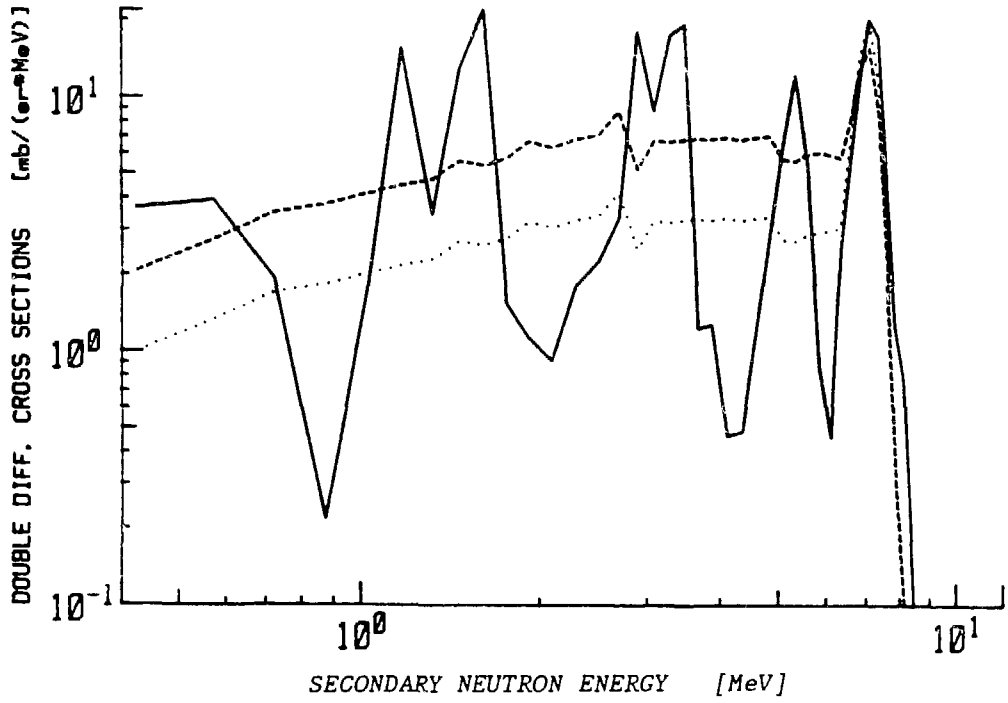

Fig. A-38. 10.0 MeV Neutrons on Boron-11 145.0 Deg.